THE MECHANISM OF RADIAL COMPRESSOR INSTABILITY

CRAWFORD DOUGLAS WINNER

1951

THE MECHANISM OF RADIAL COMPRESSOR INSTABILITY

by

Crawford Douglas Winner
Lieutenant Commander
United States Navy

Submitted to the Faculty of
Rensselaer Polytechnic Institute in Partial
Fulfillment of the Requirements for the Degree
of Master of Mechanical Engineering

Troy, New York

May, 1951

Acknowledgment

The author wishes to express his appreciation to Professor Neil P. Bailey, Head of the Department of Mechanical Engineering, Rensselaer Polytechnic Institute, Troy, New York for providing the background for a theoretical understanding of the nature of flow instability phenomena and his enthusiasm for the pursuit of a critical study of the many practical aspects of flow instabilities. The assistance of Professor James Devine and the machine shop in providing the necessary facilities of the department and in setting up the equipment is gratefully acknowledged.

The Mechanism of Radial Compressor Instability

Abstract

The limit imposed on the operating range of a radial flow compressor by surging or pulsations in the reduced flow region has long been a source of concern to design engineers who would like to use this otherwise simple, lightweight and efficient compressor.

A preliminary study of the nature of the pulsations lead to the design of the Deflected Spill Pickup in an effort to simulate the compressor flow characteristics under conditions of close control and simple analytical boundaries. A fair degree of agreement was obtained between the flow and instability characterisitcs of the spill and the actual compressor to which it was proportioned. The analysis provides an explanation for the observed differences in flow characteristics and suggests the possibilities of producing closer agreement.

During the course of the investigation it became evident that the Deflected Spill Pickup could become a valuable component in the experimental study of other flow instability phenomena by providing a source of intermediate velocity air with the flat pressure vs flow characteristics of a system closely coupled to a radial flow compressor. The work with the spill also provided the groundwork for a suggested design for a radial flow compressor that should be free of the investigated instability in the reduced flow region of operation. The tests were conducted at Rensselaer Polytechnic Institute, Troy, New York using the facilities of the Department of Mechanical Engineering.

Index

THE MECHANISM OF RADIAL COMPRESSOR INSTABILITY

INTRODUCTION

A radial compressor is designed to operate at a given flow for a given speed, that is a constant Q/n ratio, and the components such as inlet, impeller and diffuser are matched for peak performance at this design point. As the flow is reduced from the design point, holding speed constant, the discharge pressure should increase to maintain stability. In practice it is observed that the pressure curve flattens as Q is reduced (n constant) until a pulsation point is reached. This pulsation point is a definite characteristic of current designs of compressors and is shown in the typical curves of Fig. 1.

The instability which causes pulsation may occur at the inlet to the impeller or in the diffuser section. The cause of inlet instability has been thoroughly investigated and has been, in general, eliminated by proper design. Elimination of the remaining instability, while maintaining maximum performance would increase the flexibility of radial flow compressors and enhance their utility immeasurably. A review of the early work done in this field is presented by Dr. A. Stodola in Ref. 1, excerpts from which are included as Appendix B.

To date, considerable work has been directed toward the analysis and improvement of compressor performance in the useful range of operation; but yet, the limits imposed by reduced flow pulsation have been accepted as a necessary evil. The remedies as proposed

by Stodola have not been generally accepted, partly because of the loss of efficiency involved, partly because of engineering difficulties and partly due to the lack of understanding of the exact nature of the phenomenon.

It is proposed at this time to investigate the flow conditions at the entrance to the diffuser of the radial compressor in an attempt to explain the exact mechanism producing the instability. In this paper there is presented an analysis leading to the design of the Deflected Spill Pickup and a description of the tests conducted with the spill. The spill was proportioned to correspond to the General Electric Type B-1, B-2, Aircraft Turbo-supercharger compressor for which characteristic curves Fig. 1 were available from Ref. 2 for comparison. The analysis and tests are limited to the subsonic flow velocities,

$$v_t = \omega r < \sqrt{\gamma g R T_i}$$

with the working medium assumed to be air of constant γ . There is also described the use of modified deflection spill pickups for simulating compressor characteristics when using a high pressure air supply for studying other stability in flow and combustion problems; and the design of a non pulsing compressor.

The tests were conducted during the Spring Term, 1951, at Rensselaer Polytechnic Institute using the facilities of the Mechanical Engineering Department.

ANALYSIS

A system in which flow is controlled by throtling the discharge is stable if

$$dp/dQ < 0.$$

If by some means dp/dQ becomes greater than zero, the system becomes unstable and flow will either increase or decrease until a maximum or minimum pressure point is reached, at which point dp/dQ again becomes equal to or greater than zero. The system cannot remain between these maximum and minimum points, for example points A and B in Fig. 2(a).

A radial compressor operating at constant speed

$$r\omega = \text{constant},$$

generates a static pressure

$$p_i = e_i \frac{\rho_i v_t^2}{2} = \tfrac{1}{2} e_i \rho_i (r\omega)^2$$

at its impeller tips by virtue of the effect of centrifugal force. The pressure, p_i, is a maximum at $Q = 0$, where e_i approaches one. As flow increases, e_i falls off slowly due to friction losses in the impeller and throtling losses at the inlet. Therefore

$$e_i = 1 - kQ^2$$

and p_i may be represented by curve i, Fig. 3(a). If p_i were the total pressure of the compressor, the system of compressor and receiver would be entirely stable. Such a compressor, however, would have a maximum efficiency of fifty percent, the energy expended in accelerating the fluid to tip speed would be lost. To improve the efficiency of the compressor this energy in the

form of kinetic energy or dynamic pressure

$$KE = \tfrac{1}{2} m v_i^2 \quad \text{or} \quad p_K = \tfrac{1}{2} \rho_i v_i^2$$

must be recovered by diffusion .

If all the dynamic pressure is recovered by diffusion, the total pressure will be

$$p_o = p_i + p_K \qquad (1)$$

represented as line 0 in Fig. 3(a). This curve is flatter than i but at no time does the slope become positive and therefore there is as yet no indication of instability.

The velocity of the air relative to the casing as it leaves the impeller is assumed to be

$$v_i^2 = v_t^2 + v_r^2 \qquad (2)$$

where v_t is the tip speed, ωr, and v_r is the radial flow velocity relative to the impeller,

$$v_r = Q/A_c. \qquad (3)$$

The air leaves the impeller at an angle α with the tangent, see Fig. 2(b).

$$\tan \alpha = v_r/v_t = Q/A_c v_t \qquad (4)$$

and therefore, α varies with Q.

A vaned diffuser is designed to receive the air leaving the impeller at a given angle, α_D, and therefore obtains a peak performance at the corresponding design load, Q_D. The resulting pressure, p_2, of discharge from the diffuser as Q increases from Q_D is represented by line 2 of Fig. 3(a). Any instability in this region of operation would be purely a shock phenomenon not within the scope of this paper. The characteristics of curve 2 for Q

between $Q = Q_D$ and $Q = 0$ is of primary importance and the remainder of this paper will be confined to this particular region of operation. From Fig. 2(b),

$$v_i = v_t / \cos \alpha .$$

α_D is normally about 10° and for Q less than Q_D, α will be less than 10° and, hence, it will be assumed for the following that

$$v_i = v_t \doteq \omega r = \text{constant} \qquad (5)$$

It is most commonly assumed that as the flow decreases, the velocity at the throat of the diffuser decreases.

$$v_e = \frac{Q}{A_i}$$

and then

$$p_K = \tfrac{1}{2} e_K \rho_e v_e^2$$

the resulting discharge pressure

$$p_2 = p_i + p_K$$

is curve a of Fig. 3(b), which peaks at Q_m and indicates instability characteristics for $Q < Q_m$. No explanation is given for the change of velocity from v_i to v_e. If it were desired to simulate this change of velocity with a symmetrical spill pickup as illustrated in Fig. 4(a), the v_e, Q relation would be satisfied, but the external (spill) diffusion has high efficiency and little loss in total pressure. Therefore the pressure characteristics would be similar to those of a simple nozzle of identical dimensions supplied from a source of pressure p_o, Fig. 4(b) & (c). Applied to the compressor, the resultant p_2 would be curve (b), Fig. 3(b) which everywhere has a negative slope and no indication of instability. The inlet of a diffuser section as illustrated in

Fig. 5(a) may be considered an asymmetrical spill receiving excess air from a constant velocity constant total pressure source. The direction of the impinging stream is deflected by a pressure gradient that can be transmitted through the boundary layer along the outer wall of the diffuser and thus penetrate farther upstream from the lip of the spill than is possible in a symmetrical spill. This pressure acting along a greater area along the flow can produce a greater stream deflection with smaller curvature of stream lines and hence smaller transverse static pressure gradient. The part of the high velocity stream that is captured might be expected to act as a stream entering a sudden enlargement, expanding at constant momentum and loss of energy until it fills the channel, then diffusing to discharge pressure in the manner of a normal diffuser.

The idea of a simple "deflected spill pickup", Fig. 5(b) was developed to simulate the flow in the compressor. A nozzle operating from a constant pressure source providing the impinging stream at a velocity corresponding to the tangential velocity $v_t = \omega r_i$ in the compressor. With such an arrangement an analytical study could be made with the simplest boundary conditions and a working model could be built to obtain test data under conditions providing the best control.

The spill used in the present study was designed to the proportions of a diffuser section of the General Electric B-1 Aircraft Supercharger compressor for which the dimensions and Pressure vs Flow characteristics were available. The necessary dimensions are shown in Fig. 5(a) and the characteristic curves from Ref. 2

are plotted in Fig. 1. For best comparison, the spill should be made the same size as the diffuser being studied because neither Reynolds Number characteristics nor Mach Number effects can be ignored for the best accuracy. However, to accommodate the spill to the available air supply and to retain the complete velocity range, it was deemed advisable to scale down to one half size.

SPILL CHARACTERISTICS

For a preliminary analysis of the spill, assume (1) parallel flow in the discharge from the nozzle, and (2) non-viscous flow, but (3) permit the downstream pressure to penetrate two inches upstream along the deflecting wall. (The two inch value was chosen arbitrarily to illustrate the method.) Under the above assumptions the jet boundaries will remain clearly defined; the lower boundary will not entrain any free air and the boundary pressure will remain at atmospheric pressure; the upper boundary will break away from the wall at the two inch point and will be deflected by a constant pressure, ΔP_5, along the upper boundary from this point to the zero point opposite the lip of the spill; and, the total energy in the jet will remain essentially constant throughout its cross section and for its entire free length from nozzle to lip. The constant pressure, ΔP_5, acting normal to the stream will deflect the stream along a circular arc of radius, r = constant, for any particular streamline. The geometry of this flow is shown in Fig. 6, from which it can be seen that

$$r_2^2 = r_1^2 + L^2$$

$$r_2^2 = (r_2 - \Delta r)^2 + L^2$$

and solving for r_2

$$r_2 = \tfrac{1}{2}\left(\frac{L^2}{\Delta r} + \Delta r\right) \qquad (6)$$

where Δr is the amount the stream is deflected and may be written as $\Delta r = k \times b$ (7)

To determine the magnitude of the ΔP that is required to produce the curvature r_2, the differential eq. may be set up from the incremental block $dr \times r d\phi$ of Fig. 6 and radial acceleration equation

$$a_r = \frac{v_j^2}{r}. \qquad (8)$$

Using the basic force equation

$$F = ma \qquad (9)$$

$$(p + dp)\, r d\phi - p r d\phi = r d\phi dr \rho_j \times \frac{v_j^2}{r}$$

which simplifies to

$$dp = \rho_j v_j^2 \frac{dr}{r} \qquad (10)$$

For compressible flow, constant total energy, the flow conforms to the free vortex theory

$$\rho_j v_j^2 = \text{constant} = \rho_i v_i^2 = \gamma p_b M_i^2 \qquad (11)$$

and the equation (10) may be integrated to

$$\int_{p_1}^{p_2} dp = \rho_i v_i^2 \int_{r_1}^{r_2} \frac{dr}{r}$$

$$p_2 - p_1 = \rho_i v_i^2 \, \mathrm{Ln} \, \frac{r_2}{r_1} \qquad (12)$$

or with p_1 as atmospheric this gives guage pressure at point 5.

$$\Delta p_5 = \rho_i v_i^2 \, \mathrm{Ln}\left(\frac{1}{1-\frac{\Delta r}{r_2}}\right) \qquad (13)$$

Eq. (13) indicates that Δp_5 is a function of $v_i = \omega r_i$ and the dimensionless ratio $\frac{\Delta r}{r_2}$. On this basis, the spill was constructed to one half size for all linear dimensions, and it was assumed that corresponding velocities in the two systems should be equal; that is, a jet velocity of v_i in the spill would correspond to a compressor speed of $\omega r_i = v_i$. (See discussion) To put Eq. (13) in terms of the constants of the spill,

$$\Delta r = kb$$

$$r_2 = \frac{1}{2kb}\left[L^2 + (kb)^2\right] \qquad (14)$$

and from Eq. (11)

$$\rho_i v_i^2 = \gamma p_b M_i^2$$

then

$$\Delta p'_5 = \gamma p_b M_i^2 \, \mathrm{Ln}\left[\frac{1 + (kb/L)^2}{1 - (kb/L)^2}\right] \qquad (15)$$

THE DIFFUSER CHARACTERISTICS

For analysis, the action in the diffuser will be separated into into two parts, (1) the irreversible expansion of the captured portion of the jet to expand to the diffuser walls, assumed to occur in a constant area section and (2) the essentially reversible diffusion of the diffuser section. The hypothetical point 5a, Fig. 6, will be used to designate the conditions at the conclusion of the first part and the initiation of the second part of the expansion. If the spill pickup discharges through a constant cross-section, point 5a will correspond to point 6.

Between the points 5 and 5a the flow will have constant total momentum and may be analyzed in accordance with the method developed in Ref. 3 and expanded in Ref. 4.

Momentum equation:

$$\text{Mom}_t \text{ at } 5 = \text{Mom}_t \text{ at } 5a$$

$$A_i p_5 + W/g\ v_j = A_i p_{5a} + W/g\ v_{5a} \tag{16}$$

Continuity equation

$$W/g = \rho_5 A_j v_j = \rho_{5a} A_i v_{5a} \tag{17}$$

From previous development it is assumed that

$$A_j = (1 - k)\ A_i \tag{18}$$

From equation (17) and (18)

$$v_{5a} = (1 - k)\ \rho_5 / \rho_{5a}\ v_j \tag{19}$$

Substituting in equation (16)

$$p_{5a} - p_5 = (1 - k)\ \rho_5 v_j^2 \left[1 - (1 - k)\,\rho_5/\rho_{5a}\right] \qquad (20)$$

From equation (11)

$$\rho_5 v_j^2 = \rho_i v_i^2 = \gamma\ \frac{p_b v_i^2}{\gamma\, gRT_i} = \gamma\, p_b M_i^2 \qquad (21)$$

From perfect gas relation

$$p/\rho = gRT \qquad (22)$$

$$\rho_5/\rho_{5a} = p_5/p_{5a} \times T_{5a}/T_5 \qquad (23)$$

Assuming the adiabatic relation

$$T_{5a}/T_5 = (p_{5a}/p_5)^{\frac{\gamma - 1}{\gamma}} \qquad (24)$$

then

$$\rho_5/\rho_{5a} = (p_5/p_{5a})^{\frac{1}{\gamma}} \qquad (25)$$

and equation (20) becomes

$$p_{5a} - p_5 = \gamma p_b M_i^2\ (1 - k) \left[1 - (1 - k)(p_5/p_{5a})^{\frac{1}{\gamma}}\right] \qquad (26)$$

Now equation (15) expresses the relation between k and the pressure, p'_5, which produces the deflection kb; and equation (26) gives the p_5 resulting from a given back pressure, p_{5a}, and a given k. If the p_5 of equation (26) is less than p'_5 then k will tend to diminish and if $p_5 > p'_5$ then k will tend to increase. An examination of equation (26) reveals that $(p_{5a} - p_5) = 0$ at $k = 0$

and k = 1, the two extreme conditions, and it has a maximum of

$$(p_{5a} - p_5)_{max} \approx \tfrac{1}{4} \gamma p_b M_i^2$$

at

$$k \approx \tfrac{1}{2}.$$

For the case of no additional diffusion, p_{5a} may be considered constant and p_5 plotted as a function of k. Curve (1) of Fig. 7 is such a plot in which p_5 is just tangent to curve of p'_5. If the back pressure, p_{5a}, is reduced, the system will be stable at the k corresponding to the left hand intersection of these curves. If p_{5a} is raised slightly, p_5 will be everywhere greater than p'_5 and k will increase to k = 1, thus completely cutting off the flow. In fact, k can increase to $k > 1$ permitting the flow to reverse and back out the spill, unloading the receiver until p_{5a} is reduced to p'_5. k will then return to zero, full flow will resume until p_{5a} again builds up to the critical value. This sequence of events describes a phenomenon that resembles to a remarkable degree the pulsating or surging of a radial compressor that occurs when the compressor back pressure is increased beyond a critical value.

When a diffuser is added, p_{5a} can no longer be considered constant. Instead, the assumption is made that the discharge pressure p_6 is constant. Then for a reversible diffusion to negligible velocity, see Ref. (3),

$$p_6/p_{5a} = \left(1 + \frac{\gamma - 1}{2} M_{5a}^2\right) \frac{\gamma}{\gamma - 1} \qquad (27)$$

or put in the coordinates of Fig. 7.

$$\frac{\Delta p_{5a}}{\gamma p_b M_i^2} = \frac{\dfrac{p_6/p_b}{\left\{1 + \left[(\gamma - 1)/2\right] M_{5a}^2\right\}^{\frac{\gamma}{\gamma - 1}}} - 1}{\gamma M_i^2} \qquad (28)$$

A typical curve representing this flow is Δp_{5a} (3) and its corresponding Δp_5 (3) which shows no minimum between k = 0 and k = 1. This indicates that so long as p_6 is below the critical value, the flow is stable and k will remain equal to zero. As p_6 is increased past the critical value, the system will go unstable and pulsations will commence as before, but without any jet deflection before complete breakdown occurs. The curves Δp_{5a} (2) and Δp_5 (2) represent a typical case with an intermediate degree of diffusion. The curves of Fig. 7 indicate that a compressor with ideal diffusion would always go unstable when the back pressure reduced the flow below

$$Q'_{minimum} = nA_i \; r\omega \; \rho_i/\rho_b \qquad (28)$$

but from forced vortex theory,

$$\rho_i/\rho_b = (p_i/p_b)^{\frac{1}{\gamma}} = \left[1 + \frac{\gamma - 1}{2} \frac{(\omega r)^2}{\gamma g R T_o}\right]^{\frac{1}{\gamma - 1}} \qquad (29)$$

then

$$Q'_{minimum} = nA_i \; r\omega \left[1 + \left\{\frac{\gamma - 1}{2} \frac{(\omega r)^2}{\gamma g R T_o}\right]^{\frac{1}{\gamma - 1}} \qquad (30)$$

in which n represents the number of diffuser sections, A_i the same as before, and the last term is to standardize Q to atmospheric pressure and temperature. This $Q'_{minimum}$ is valid for diffusion

somewhat less than ideal complete diffusion, but as degree of diffusion is reduced further, $Q_{minimum}$ will reduce to a value such that

$$Q_{minimum} \cong 0.4\, Q'_{minimum} \tag{31}$$

A close examination of Fig. 7 shows that the theory predicts a flattening of the pressure curve as flow increases from Q'_{min} to Q_{min} with a discontinuity in the slope at Q'_{min} and zero slope at Q_{min}. Increasing the slope of p'_5 to p''_5, shown in Fig. 7 as a dotted line would extend the flattened portion of the characteristic to lower values of Q; and, increasing p'_5 to p'''_5 will permit stable operation down to zero flow.

A discussion of some of the defects and limitations of the above analysis, not already pointed out, is included in the general discussion of results of the tests.

EQUIPMENT AND PROCEDURE

EQUIPMENT

A Deflected Spill Pickup was designed on the proportions of a diffuser section of the General Electric B-1 Aircraft Turbo-supercharger, Fig. 5(a), with the linear dimensions scaled to one half size. Fig. 8 is a drawing of the spill, with dimensions. The square nozzle was shaped to an ellipse of semi axis 1" X $\frac{1}{2}$", and with $\frac{1}{4}$" parallel sides at the minimum cross section of $\frac{1}{2}$" X $\frac{1}{2}$" square. The nozzle was cut from brass, and the spill was of brass stripping. The main diffuser corresponds to the diffuser vanes of the compressor and the diffuser extension to the diffusion provided by the compressor casing. Three different diffuser extensions shaped from galvanized iron sheet were used for various tests. The spill was provided with three static pressure taps along the upper surface, and static and total pressure probes were inserted through the open bottom of the spill for obtaining operating pressure surveys. The outside diameter of the probes was .05", the orifice in the total head tube was .0292" diameter and the two orifices in the static head tube were .0135" diameter. The tubes were mounted in a precision tool carriage for positioning.

Air for the tests was provided by a Schramm Air Compressor of 100 cfm capacity at 80 lb/sq. in. driven by a 50 HP, 1175 RPM Westinghouse induction motor. The compressor is provided with a small aftercooler which helps to hold down the operating temperature, but does not provide any accurate temperature control. A large

surge tank is provided for smoothing the flow from the compressor and an unloader valve prevents excess pressure. A one inch supply line from the surge tank fed the air to the test system pictured in Fig. 9, 10, 11 and 12. The by-pass valves were provided to adjust the flow so as to hold the pressure in the surge tank constant at some pressure below the unloading pressure. The 3/4" primary metering nozzle in the high-pressure receiver was used to check the flow through the main nozzle and by this means it was possible to confirm that the main nozzle was flowing full. The plenum chamber was constructed of 26 guage galvanized iron sheet and had a volume of 7.5 cu. ft. ahead of the 1.5 inch metering nozzle and 4.5 cu. ft. between metering nozzle and the two inch globe valve used as the exhaust control valve exhausting to the atmosphere. A Weston, clock dial, stream thermometer was used to obtain the total temperature in the receiver chamber. All other data on the runs was obtained as static pressures. The receiver pressure was measured with a mercury manometer. The plenum chamber pressure was measured with a mercury manometer except for the runs with the third diffuser extension when a water manometer was used. A water differential manometer was used across the primary metering nozzle, and a three inch inclined differential manometer was used across the plenum chamber metering nozzle. A water manometer was used to measure the pressures in the spill.

PROCEDURE

The runs were made by setting the receiver pressure to hold steady at a given pressure while the flow through the plenum chamber was varied with the exhaust valve. Readings were taken with the exhaust valve wide open, with the exhaust closed to the verge of pulsation in the spill, and with enough intermediate settings to establish the shape of the curves. The determination of a complete curve at one setting of the receiver pressure constituted a single run. It was established that the direction of approach to a point did not affect the readings obtained, even near the pulsation limit, and that test results were reproducible to the accuracy of the measurements. The apparatus was very sensitive to barometric changes and to variations in the total temperature in the high pressure receiver. For this reason, the barometric pressure was read before and after each run, and the total temperature read for each test point. Each run was completed in the shortest time possible so that it would be reasonably valid to use the mean barometer and temperature readings; otherwise, the test points for one run would correspond to a range of compressor speeds. The runs in which these variations affected the results were discarded and the run repeated under more consistent conditions. It was observed during the course of the tests that the receiver total temperature could be controlled over a small range, such as for holding the temperature to a single value after the system was warmed up, by skillful juggling of the control valve and by-pass valves.

Prior to the runs, the approximate receiver pressures to

correspond to a good spread of compressor speeds were determined. These pressures were used throughout the runs, and the exactly corresponding compressor speeds computed afterwards.

The data tabulated for each test point is:

to - Receiver temperature, ^{o}F

Δp_0 - Receiver guage pressure, in. Hg.

Δp_1 - Differential pressure across primary metering nozzle, in. Water

Δp_2 - Plenum chamber guage pressure, in. Hg. except for runs (13), (14) and (15), in. Water.

Δp_3 - Spill nozzle

Δp_4 - Spill center

Δp_5 - Spill Opposite lip

Δp_6 - Probe

} Attached to single water manometer through manifold and cocks; in. water, guage

Δp - Differential pressure across plenum chamber metering nozzle, inclined manometer scaled to .01 in H_2O.

The limiting run with these guages was with a receiver pressure of 16 inches of mercury, corresponding to a compressor speed of 17,600 RPM. When the guages were secured and the receiver pressure run up to 18.5 inches Hg, corresponding to 20,000 RPM, the pulsations were extremely violent, causing the plenum chamber walls to buckle and air to puff through at the joints. Therefore, it was not considered necessary to obtain guages with higher pressure ranges. It is believed that the range of runs obtained is sufficient for the present purpose of the tests.

The probes were only inserted for runs #9 and #11 which were specifically for the purpose of obtaining typical pressure profiles. For these runs, the flow was adjusted to as close to the pulsation point as possible and then increased .01 inches on the inclined manometer to eliminate the possibility of pulsation during the surveys. The probe did not appreciably affect the maximum pressure before pulsation, but the flow had to be decreased about .02 inches to maintain the same pressure as before the probe was inserted. The probes were mounted on a precision tool carriage which had horizontal scales marked to .025 inch. The surveys were made along the lateral centerline of the spill, positioned upstream from the lip of the spill as the zero longitudinal position, and positioned vertically down from the position against the top wall as the zero, with an adjusting knob, 14 turns of the knob moved the probe one inch and readings were taken every half turn. The forward projection of the total head tube was 0.16 inches thus making this the minimum horizontal position for this measurement. The static head tube could be pointed in either direction and give consistent results, thus making it possible to obtain static readings at the zero horizontal position.

Difficulty was experienced in completing a pressure survey without bending the tube sometime during the run against either the top or the lip.

Sample computations are included in Appendix A.

RESULTS AND DISCUSSIONS

Tests with the Deflected Spill Pickup proved very dramatically that the design will produce pulsating flow similar to that experienced in radial flow compressors. With the pickup discharging into the relatively large plenum chamber, it was possible by adjusting the discharge, to control the rate of pulsation down to about three per minute; slower than this, the rate became erratic and seemed to depend on occasional fluctuations of supply pressure. Therefore, this rate was taken as pulsation point and the relatively steady conditions just prior to each pulse was taken as the limiting values for the tabulated readings. Each pulse occurred very abruptly and without warning, discharging the primary jet plus the excess air from the plenum chamber out the bottom of the spill, then returning to normal flow. The test spill also provided evidence as to the source of much of the noise of a compressor. Operating at speeds corresponding to about 5,000 RPM and less, the noise level of the laboratory was not increased appreciably. Above that speed, the noise level increased until at 18,000 RPM it was extremely uncomfortable, even with good ear plugs. As the speed or rate of discharge was adjusted, various frequencies came into resonance, but in general most of the noise could not be identified as having any particular pitch.

The data obtained from the runs, together with the important computed values for each run are presented in Tables I through XI. Sample computations for these tables are included as Appendix A. The results are presented graphically in Fig. 13

through 16 as pressures vs a standardized flow rate which is computed as described in Appendix A. Where possible, the run number is used to identify the curve.

Fig. 13 is a direct plot of the plenum chamber guage pressure, Δp_2, and Fig. 14 is a direct plot of spill deflecting pressure, Δp_5. The series of curves on both these plots exhibit a consistency of results as the operating pressure is increased. The Δp_2 curves have definite breaks in slope at the Q for which the Δp_5 becomes zero; this is the Q'_{min} described in the analysis. Runs (3), (4), (5) and (6) were consistent in pulsating at about two-thirds Q'_{min}. (7) and (8) pulsated at higher percentages of Q'_{min}. Actually, the diffusion efficiency was higher in these runs (probably due to effect of increased N_R) and therefore this is still consistent with prediction as is the low Q_{min} of run (15) with no diffusion. The sharp break in the Δp_2 curve of run (10) is probably the result of compression shock losses as Δp_5 has dropped low enough to produce supersonic flow in the spill in this region. The theoretical curve of $\Delta p'_5$ corresponding to runs (6), (12) and (15) is plotted as a dotted line in Fig. 14. The theoretical curve was computed for a constant value of L = 1.0 inch. A comparison of the actual curves with the theoretical indicates that, in practice, L is not a constant, but is a function of the stream deflection, k, starting at zero for k = 0 and increasing in an almost linear manner with k. The intersection of the theoretical with the actual should indicate the flow at which the effective L = 1 inch.

The $\Delta p'_5$ of run (6) is plotted as a dotted line in Fig. 7 to illustrate how the variation of L effects the theoretical stability. It can be seen immediately that the curve is becoming parallel to curve $\Delta p_5(2)$ at the point of instability and that as curve $\Delta p_5(2)$ is translated vertically, the point of tangency would occur at this point. $\Delta p_5(2)$ is the theoretical curve corresponding to a system with partial diffusion. The effect of the negative curvature of $\Delta p'_5(6)$ is to increase p_2 to a higher and sharper peak with a shorter region of small dP/dQ.

To compare the results with the compressor curves of Fig. 1, the guage pressure Δp_2 was converted to pressure ratio and increased by a factor representing the static pressure at the impeller rim. The Q was then corrected across this pressure rise to a new Q of standard atmosphere and increased by a factor of four to correct for the reduced scale, and a factor of seven to account for the seven diffuser sections in the compressor. The results are plotted in Fig. 15 with an overlay of the actual compressor curves for comparison.

The test curves in general fall somewhat below the compressor curves. After this was observed, an analysis of the diffuser action was made and this revealed that the diffuser was almost totally ineffective. The original diffuser extension was replaced by a longer diffuser extension with maximum total angle between opposite sides of 5°. Runs with this extension showed a slight increase in p_2, see curve (12) in Fig. 13 and 15, but an analysis of the diffuser action again showed very poor efficiency at the intermediate speeds.

When the main diffuser was scaled down from the size of the diffuser vanes in the compressor, the linear proportions were preserved including the angle of divergence, and it was possible to preserve the area ratio by virtue of the parallel vertical sides, but this similarity is not sufficient. For our purpose, it was not feasible to increase the velocity to preserve dynamic similarity and therefore, the length should have been longer to hold down the linear pressure gradient. A second contributing factor in the poor diffuser performance is the square corners in the diverging channel. There is no doubt that the high linear pressure gradient combined with the poor flow conditions in a cross section having sharp, square corners combined to cause flow separation and poor diffuser efficiency.

Similarly, in the analysis justifying the linear proportioning of the spill, the effect of Reynold's Number along the upper (deflecting) wall was neglected. Actually, the development of boundary layer on the wall is a function of N_R, and the penetration, L, of the deflecting pressure along this wall is undoubtedly affected by the degree to which the boundary has been developed. Therefore, if the length of this wall is reduced from the original length, the jet velocity must be changed to preserve dynamic similarity. Such a change, however, will involve conversion factors for correcting velocities and pressures to the corresponding compressor speeds. As a result, the beauty of simplicity is lost. These corrections factors can be established if such accurate results are found of value. The neglect of this effect is evidenced in the curves of Fig. 15 as a slightly steeper slope of the test curves over the compressor curves.

The assumption of non-viscous flow in the analysis of the jet deflection is obviously one of expediency. It cannot predict the distance L; however, with the proper value of L, the overall effect of the hypothetical flow is in good agreement with the observed effect. The results of the pressure survey are plotted in Fig. 16 and indicate that the flow more closely resembles that of a free vortex as modified by the deflecting wall. Any further analytical development would probably follow along such lines.

USES FOR THE DEFLECTED SPILL PICKUP

In gas turbine applications and jet engine designs some flow instabilities have been observed to occur prior to compressor instability and within normal combustion limits. Laboratory study of the phenomena has been hampered by the fact that no air supply other than a closely coupled radial compressor had been found that has the flat pressure-flow characteristic at intermediate flow velocities. The deflected spill with an efficiently designed diffuser to bring the flow to the desired discharge velocity and pressure appears to be the answer to the supply problem. By properly adjusting the primary jet velocity and diffuser area ratio, any desired combination of discharge velocity and pressure may be brought to the flat portion of the characteristic curve. As previously explained, this flat portion can be appreciably extended if the $\Delta p'_5$ curve can be made to be concave upward, and this can be accomplished by any device that will hold the deflection point L at some definite point ahead of the lip of the spill. Several suggestions for such devices are presented in Fig. 17. After a discussion with this author, the configuration of Fig. 17(d) was developed by Mr. Robert Edelman as a modification to a symmetrical spill pickup during his work on combustion stability. It is described in more detail in his thesis, Ref. 5. There is no need for the deflecting wall to be rigidly attached to the nozzle as was done in the original model.

THE DESIGN OF A PULSELESS RADIAL FLOW COMPRESSOR

The preceding development and discussion describes the mechanism which appears to be responsible for the pulsations observed in a radial flow compressor as the flow is decreased by back pressure. If such is the case, then it also contains the essential information for the design of a compressor that may be free of discharge instability for all rates of discharge from the designed rate to a zero rate of discharge. The above is restricted to the case of subsonic impeller tip speeds, but the essential features should apply to the supersonic case with only slight modification of channel design to improve the efficiency.

The last page of the Analysis, referring to Fig. 7, points out that if the slope of curve $\Delta p'_5$ can be increased to $\Delta p'''_5$ then there will be no point of instability as the flow is reduced to zero. Curve $\Delta p'''_5$ corresponds to a small value for L. If the deflecting wall were removed completely, then L would be zero and the condition would be satisfied. The mechanism producing instability would be removed. The resulting diffuser inlet would correspond to a symmetrical spill pickup and tests have shown that such a device will go to zero flow at a pressure corresponding very closely to the total pressure in the impinging stream, and with complete stability; in fact, such a device is the Pilot tube.

The symmetrical spill diffuser might take the configuration shown in Fig. 18. The diffuser section is essestially the same as in present designs, but there is a break in the outer wall through which air is bled back to the side of the impeller

housing at the tip of the wheel. The purpose of this bleed is not to maintain the total flow above the originally critical flow, but to prevent a deflecting pressure from being transmitted along the outer side of the channel. The maximum conceivable cross section for such a bleed would be one half the cross section of the diffuser inlet, but by proper design at the pickup end and at the discharge end, it may be possible to cut this size to less than one fifth. At design flow rates and higher the effect on compressor efficiency should be negligible, and at lower rates, the efficiency should be improved.

The author intends to continue development and test work on the design and is requesting that Navy facilities be made available for this work.

CONCLUSION

From these tests and analyses, it can be concluded that:

1. The deflected spill pickup has flow instability characteristics similar to those of a radial flow compressor with vaned diffuser.
2. The deflected spill pickup may be proportioned to reproduce the constant speed pressure vs flow characteristics of a specific radial flow compressor having a vaned diffuser.
3. The deflected spill pickup may be proportioned to provide a supply of air at any given intermediate velocity with an algebraically larger dp/dQ than is normally available from any source other than a closely coupled radial compressor.
4. The source of the most troublesome radial compressor pulsations, which determine the lower flow limit at a given speed, is the region at the entrance to the diffuser vanes.
5. The source of these pulsations can be eliminated with negligible loss in efficiency, by converting the entrance to the diffuser section to correspond to a symmetrical spill pickup as described in the above discussion.

SAMPLE COMPUTATIONS

1. For measuring the primary flow through the .75 inch, long radius metering nozzle.

   (a) For Δp_1 less than $16"H_2O$

$$W = A\sqrt{\frac{2g}{RT}\ p_o\ (\Delta p_i)} \qquad g = 32.2\ ft/sec^2$$

$$R = 53.35\ ft\ lb/^oR$$

$$W = .0645\sqrt{p_o("Hg)\,\Delta p_1("H_2O)/T_o(^oR)} \quad lb/sec$$

   (b) For $\Delta p_1 > 16"H_2O$

$$p_o/p = 1 + \frac{.0735\ \Delta p_1("H_2O)}{p_2\ ("Hg)}$$

Determine M_1 and $F = \frac{W\sqrt{T_o}}{Ap}$ from Table of Functions of Mach number for air from Ref. 3.

$$W = \frac{FAp}{\sqrt{T_o}} = 0.26\ \frac{P_2\ ("hg)F}{\sqrt{T_o\ (^oR)}}\ lb/sec$$

2. Similarly for plenum chamber 1.5 in. metering nozzle, all non-compressible,

$$W = .0258\ \sqrt{P_2("Hg)\ \Delta P_7("H_2O)/T_o(^oR)} \quad lb/sec$$

3. The static temperature of the jet T_i determined from the Tables of Ref 3 and then,

$$v_i = M_1\sqrt{\gamma gRT_i} = 49\ M\sqrt{T_i}\ \ ft/sec$$

4. The corresponding compressor speed is;

$$N = 60\ \frac{\omega}{2\pi} = \frac{60}{2\pi}\ \frac{r\omega}{r} = \frac{60}{\pi D}\ v_i$$

for D = 11.5" = .958

$$N = 19.9\ v_i \quad RPM$$

5. The equivalent compressor compression ratio is

$$(p_2/p_1)_c = (p_i/p_1)_c \, (p_2/p_i)$$

where (p_i/p_1) is the static pressure at the impeller tips. At the lower flow rates that are of most importance $(p_i/p_1)_c$ is equal to the velocity head with only slight error hence it was assumed for this computation that $(p_i/p_1)_c = p_o/p_3$. For the second factor, p_i is assumed to be p_b, then

$$(p_2/p_1)_c = (p_o/p_3)(p_2/p_b)$$

6. The Q_c of the compressor is based on inlet air at 59°F not on the static pressure at the impeller tip, therefore, to standardize the Q of the spill to the conditions of the equivalent compressor it is necessary to take into account the effect of this additional compression. It is also necessary to take into account the scale factor of 4 for the area ratio and a factor of 7 for the number of diffuser sections in the compressor, then

$$Q_c = 60 \times 28 \, \frac{W_2 R}{p_1} \, T_1 \sqrt{\frac{T_{std}}{T_1}} = 1680 \, R \sqrt{T_{std}} \, \frac{\sqrt{T_1}}{p_1} \, W$$

$$= 2.04 \times 10^6 \, \frac{\sqrt{T_o (T_i/T_o)^2}}{p_b \, (p_3/p_o)} W = 2.04 \times 10^6 \, \frac{(p_o/p_3)\sqrt{T_o}}{p_b \, (T_o/T_i)}$$

or converting to p_b in ("Hg)

$$Q_c = 28{,}900 \, \frac{(p_o/p_3) \sqrt{T_o(^\circ F)}}{(T_o/T_i) \, p_b(\text{"Hg})} \quad \text{cu ft/min}$$

7. For plotting data not concerned with the equivalent compressor, the Q is standardized to p_b and T_o corrected to standard conditions of p_b = 29.92"Hg and t_o = 80°F.

(a) If the ordinate is (p_2/p_b)

$$f(p_2/p_b) = M = \frac{v}{T} C'$$

$$Q = vA$$

$$Q_s = 60 \frac{WRT_o}{p_b} \sqrt{T_{std}/T_o}$$

$$= 1050 \frac{W_2 \sqrt{T_o(^\circ F)}}{p_b \text{ ("Hg)}}$$

(b) If the ordinate is Δp

$$\Delta p = \frac{p}{2gRT} v^2$$

$$Q = vA$$

$$Q_s = 60 \frac{WRT_o}{p_b} \sqrt{(T_{std}/T_o)(p_b/p_{std})}$$

$$Q_s = 192 W \sqrt{T_o(^\circ F)/p_b(\text{"Hg})}$$

APPENDIX B

THE CENTRIFUGAL COMPRESSOR SURGING AND ITS PREVENTION*

A phenomenon which, as a mysterious difficulty has in the beginning given builders of centrifugal compressors no end of worry, is "surging"; that is, a periodic sudden sending back of the compressed air through the compressor into the atmosphere. The impact of the jet opposing the rotation on the blades was in many cases so great that the blades were bent or broken. The cause of the surging is the instability of the dynamic equilibrium on the rising branch of the characteristic curve. The process is as follows, see Fig. B-1.

The compressor is started with the pressure reservoir empty. As the r.p.m. increase the terminal pressure rises along a parabola b, until at A the normal condition of operation has been reached. If the regulation is for constant r.p.m., then with decreasing flow, Q, the condition approaches the point A_m. Suppose that equilibrium has here been established. Now, let the air consumption suddenly drop to $Q_x < Q_m$. In consequence of the slight throttling taking place, the flow of the air is retarded and the quantity drops. It cannot remain, however, at Q_x, because at this quantity the pressure generated is $p_x < p_m$. The quantity therefore sinks back to zero, and the discharge pipe is emptied with the initial pressure difference $p_m - p_a$ in the suction pipe. When p_a has been reached, the flow (on account of the slight acceleration

*Quoted from "Steam and Gas Turbines", Sect 208 (7) by Dr. A. Stodola, McGraw-Hill, N. Y. 1927.

of the machine that has occurred in the meanwhile) begins anew and keeps increasing since, when Q_x is reached the pressure generated is $p_x > p_a$, so that the delivery rises under the unusually powerful acceleration in the air column in an extremely short time, during which $p = p_a$, to Q_b with the condition B. The governor provides for necessary higher output, and the discharge pipe is filled, so that with decreasing quantity, A_m is reached again, from which point the process is again repeated.

A remedy is usually found in the so-called relief valve, which actuated by the quantity delivered establishes a connection between the discharge pipe and the suction pipe as soon as the quantity falls below the breakdown point. The opening of this relief valve must be so proportioned that exactly the proper quantity is blown off as is necessary to keep the compressor operating above its breakdown point; that is, if Q_x in Fig. B-1 is the useful quantity, the quantity ΔQ_x must be blown off. Another means with somewhat better efficiency is by throttling the inlet, whereby for each quantity below Q_m a new characteristic curve with a lower peak comes into play, so that with a slightly reduced pressure, stable operation becomes possible even down to zero. The best remedy would be to regulate the diffuser inlet for area and angle so as to get always shockless inlet. By reducing the diffuser width and the blade angle, operation without shock may be established for the quantity Q_x. resulting in the steep pressure line, the peak of which is to the left of point C_x, so that operation free from surging with a materially better efficiency than before becomes possible.

An entirely different method is pursued by the Allgemeine Elektrizitatsgesellschaft. A pipe of reduced diameter and of a definite length is attached directly to the compressor, and at the beginning of the surging period the pipe offers an increased inertia resistance and raises the surging frequency of the compressor. The dampening pipe is so computed as to bring the pressure oscillations in the compressor and in the pressure piping into interference, so that there is practically no noticeable oscillation.

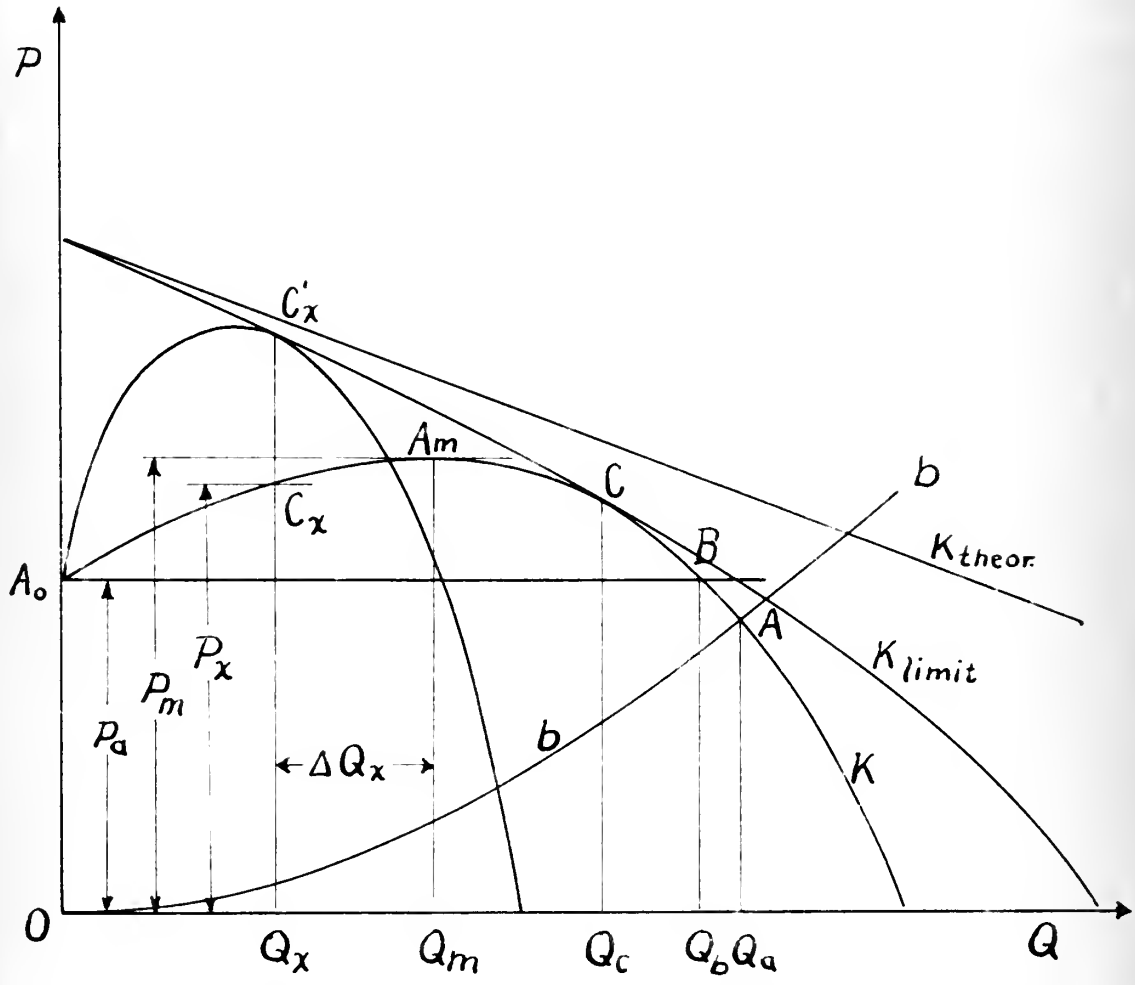

FIG 1093 — SURGING AND ITS PREVENTION

FIG. B-1

FIG 1

COMPRESSOR TYPE B-1, B-2 GE

(REF. 2)

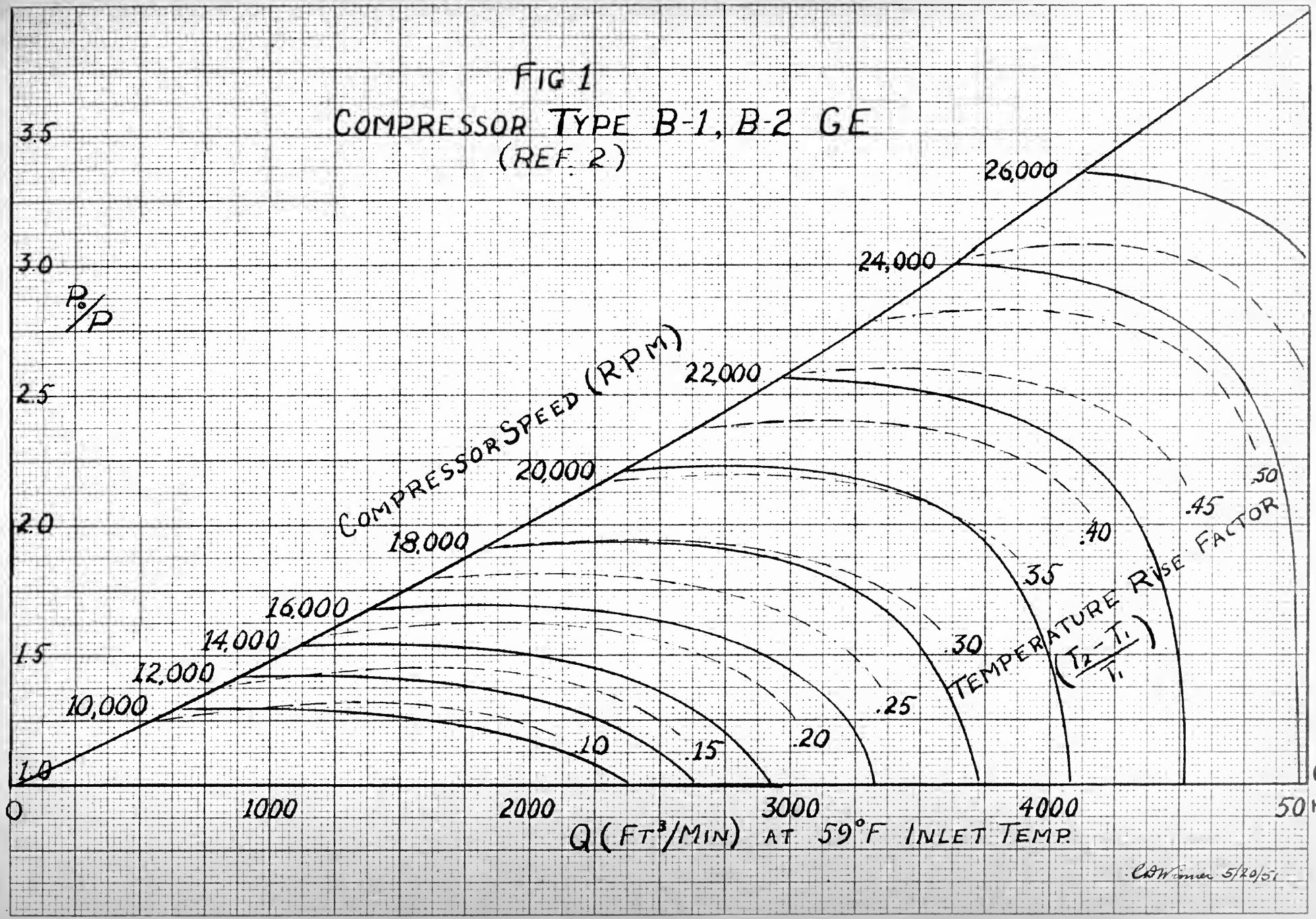

C-1

C.D. Winer 5/20/51

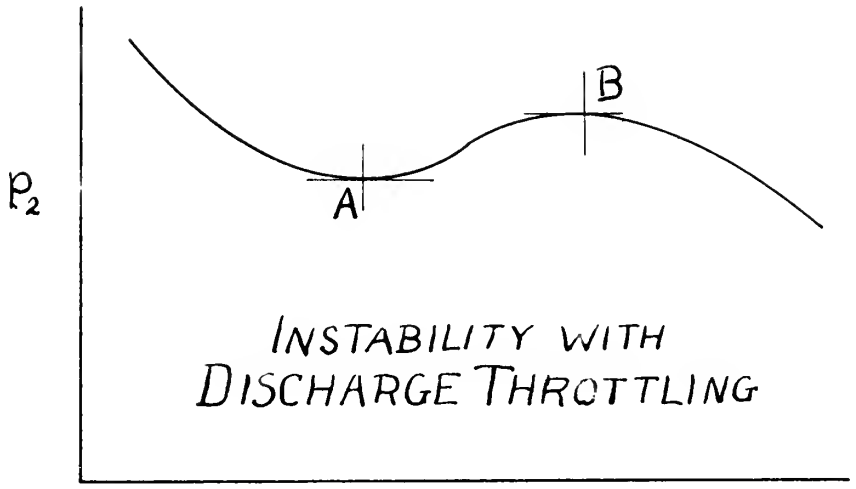

2(a)

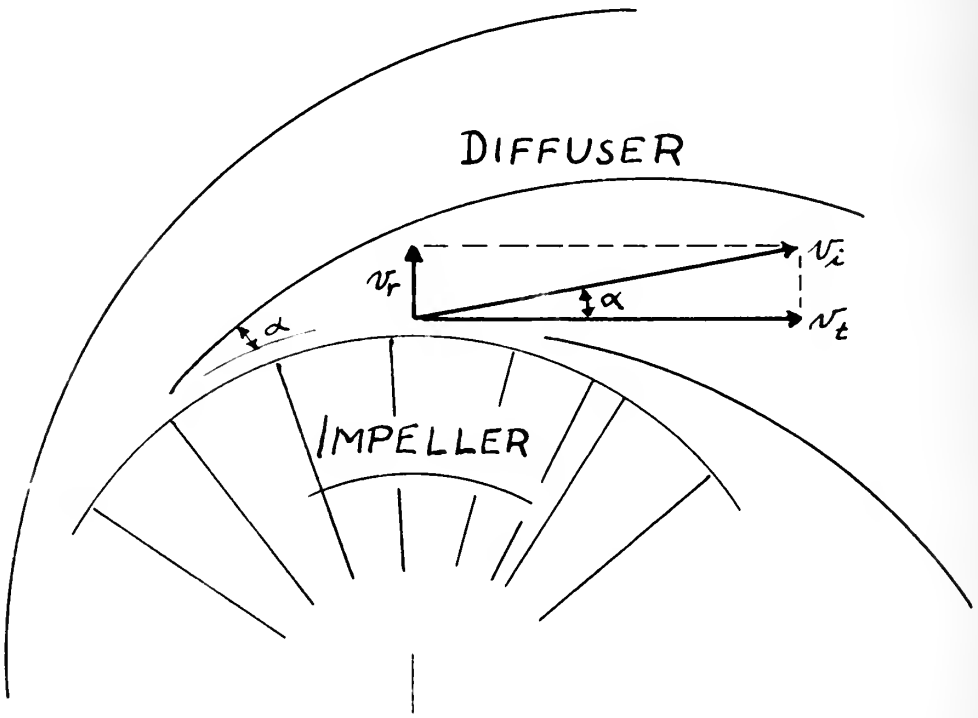

2(b)

FIG 2

E.W. Kimm 5/21/51

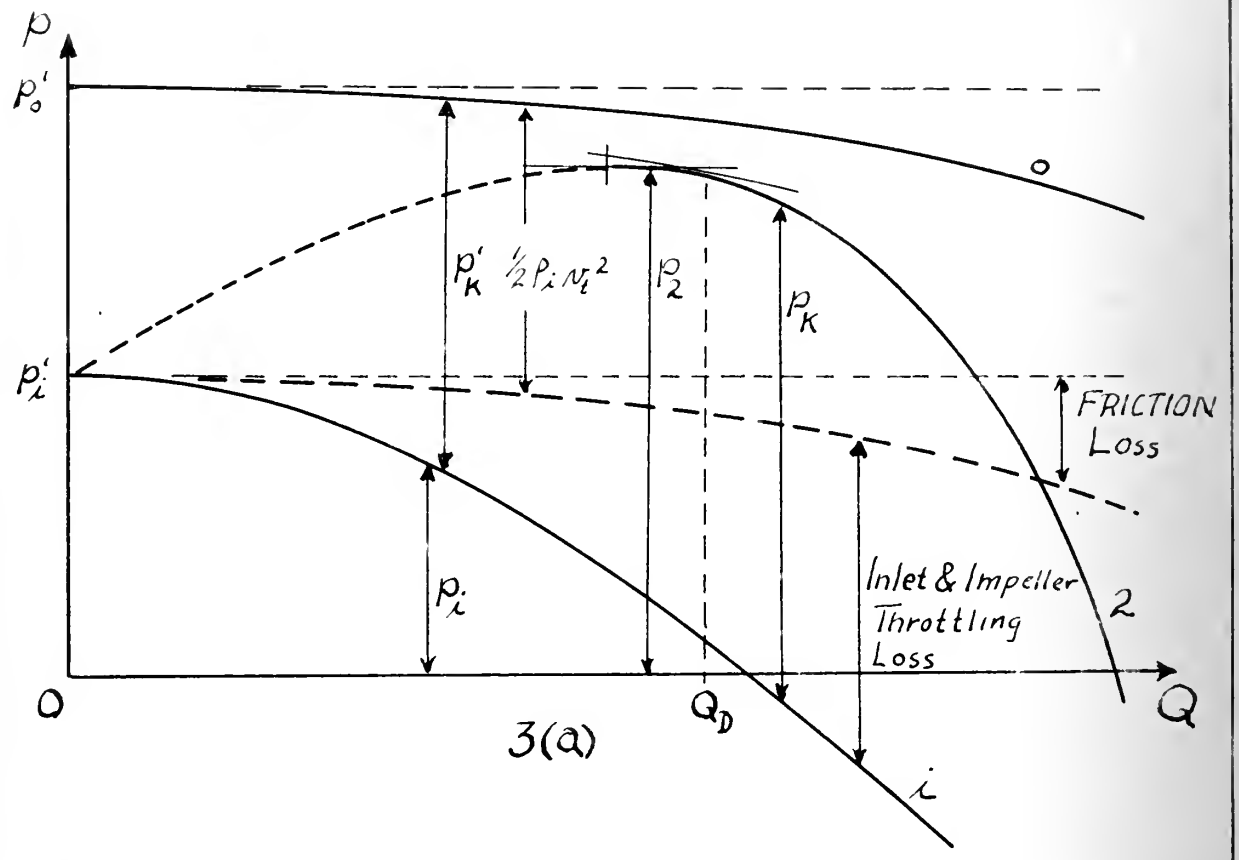

3(a)

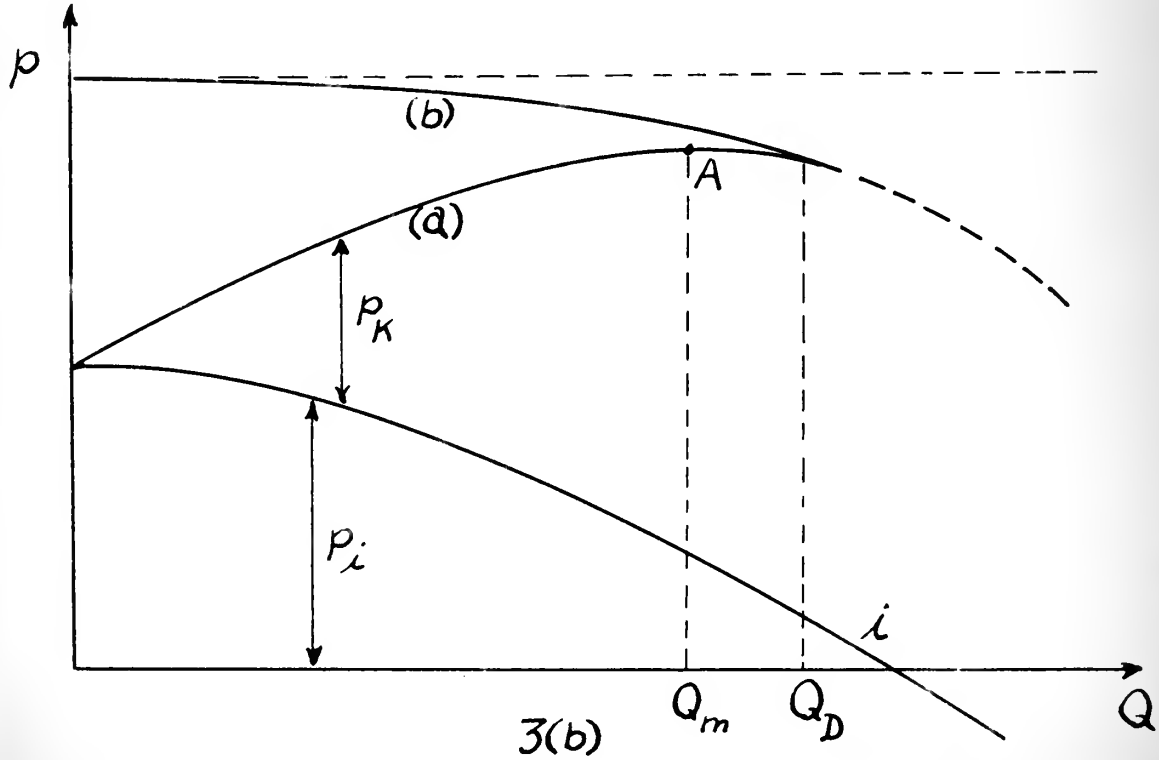

3(b)

FIG 3

L. D. Wimmer
5/22/51

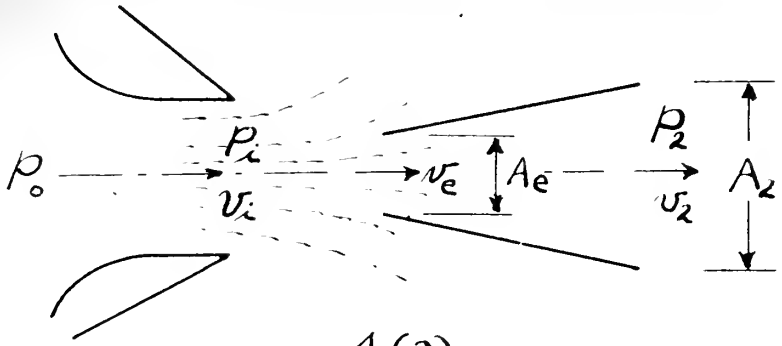

4(a)

SYMMETRICAL SPILL PICKUP

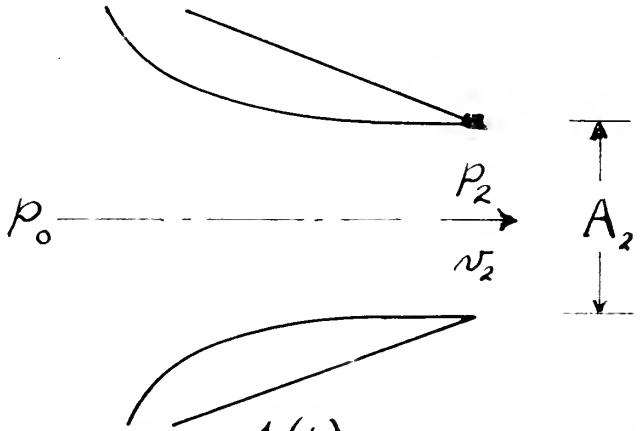

4(b)
SIMPLE NOZZLE

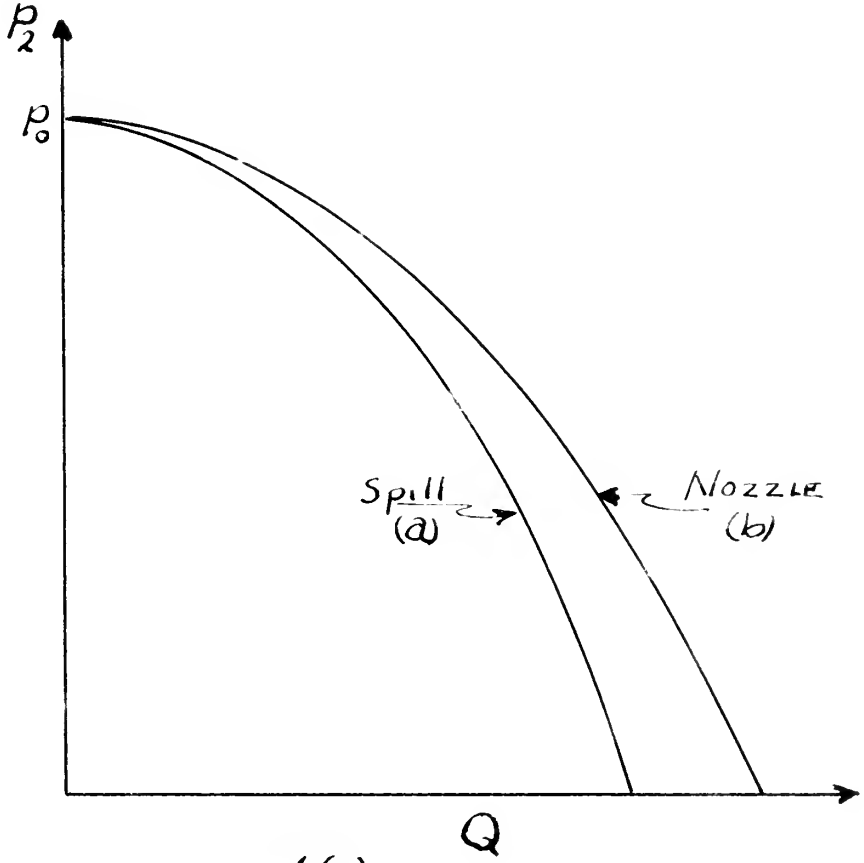

4(c)
FLOW CHARACTERISTICS

FIG 4

C-4

W Zimmer 5/22/51

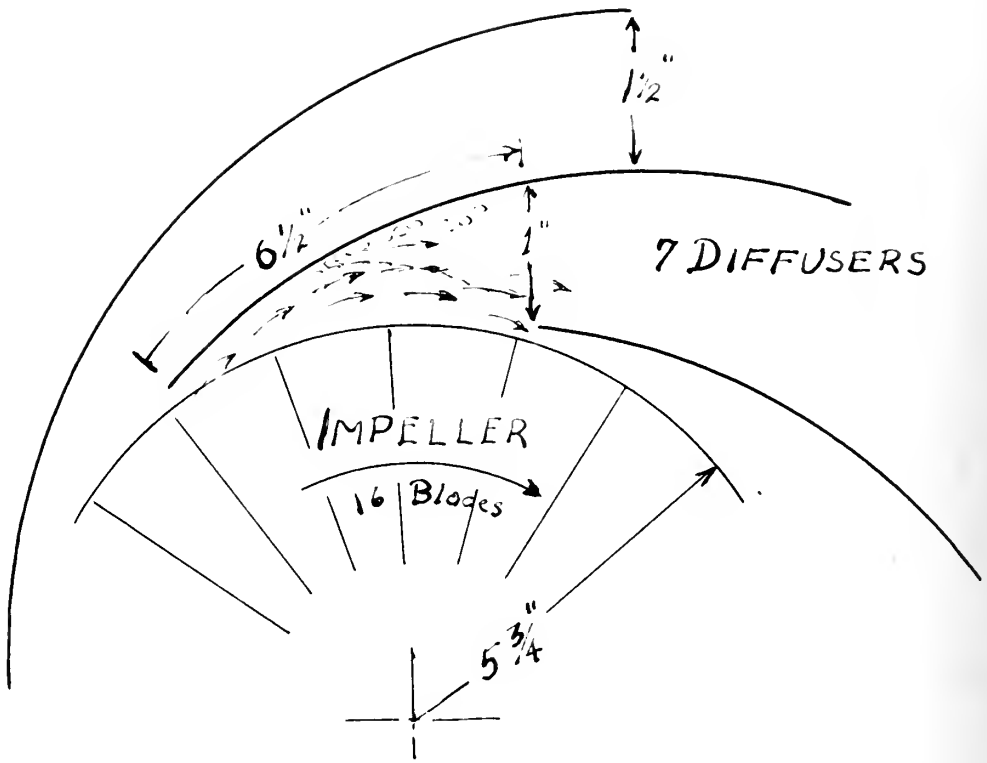

(a)

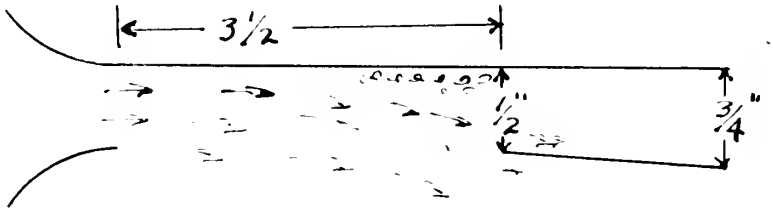

(b)

FIG 5

C. R. Rimmer 5/53

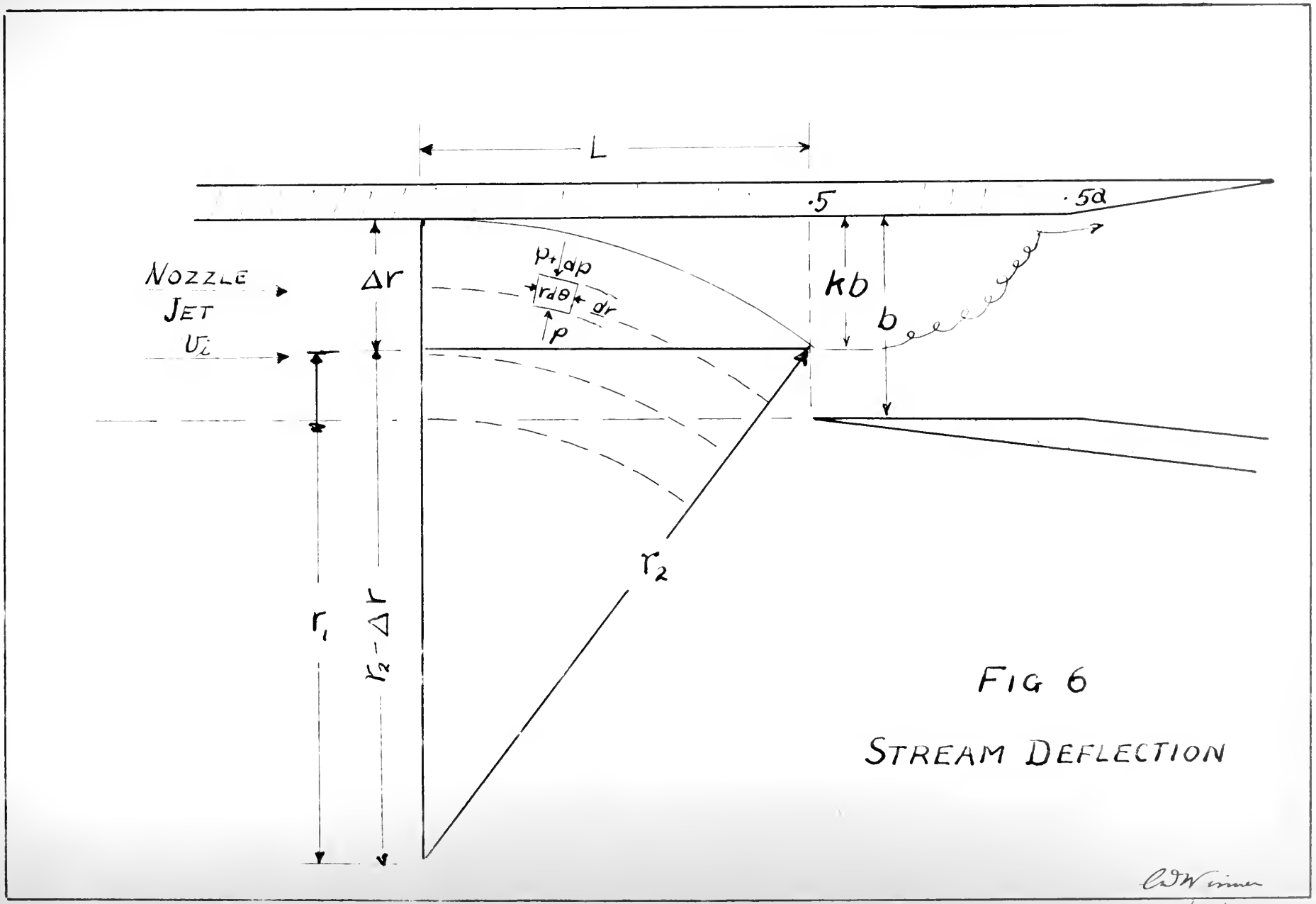

FIG 6

STREAM DEFLECTION

C.W. Simmons
5/23/51

FIG 7
ANALYTICAL SPILL

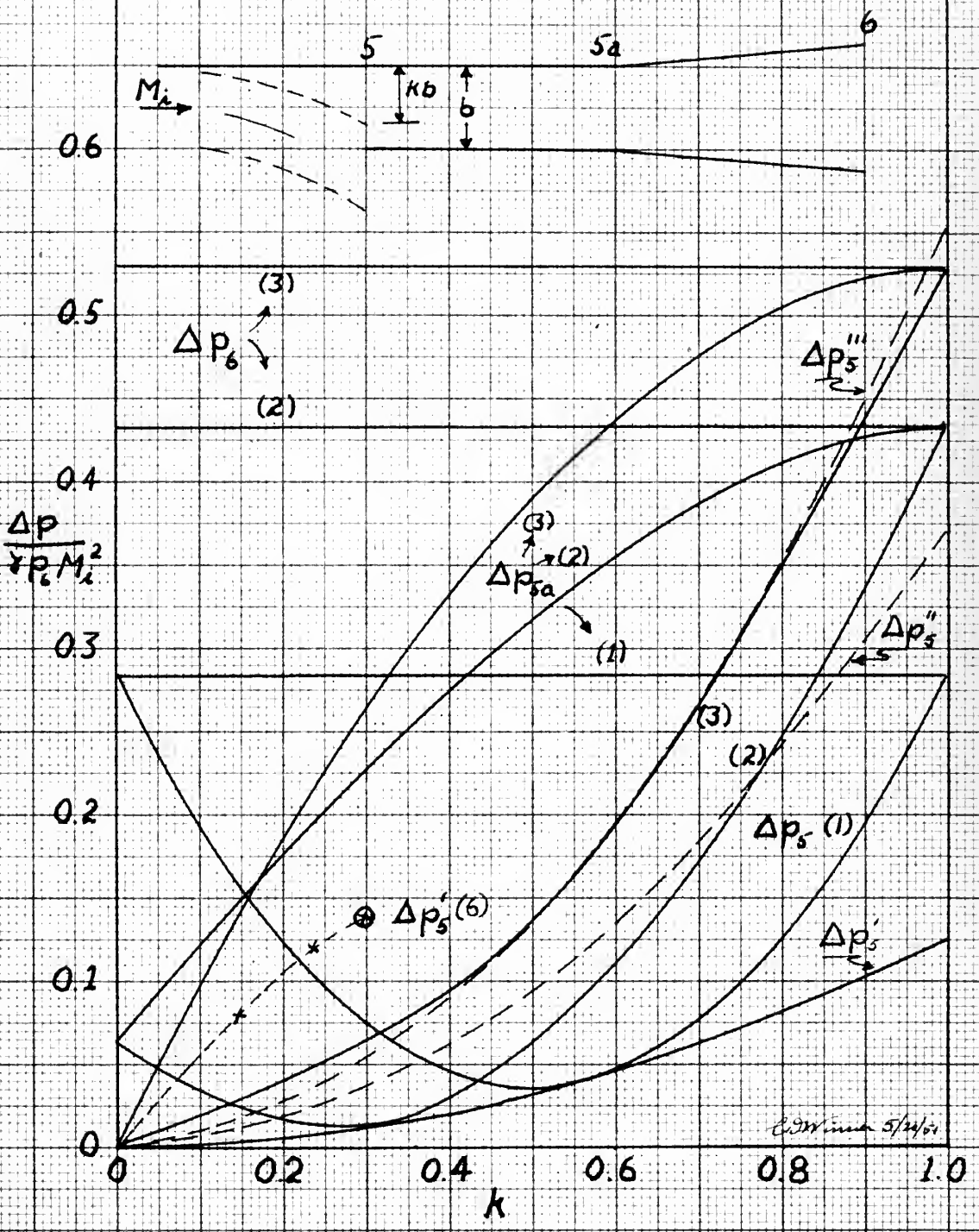

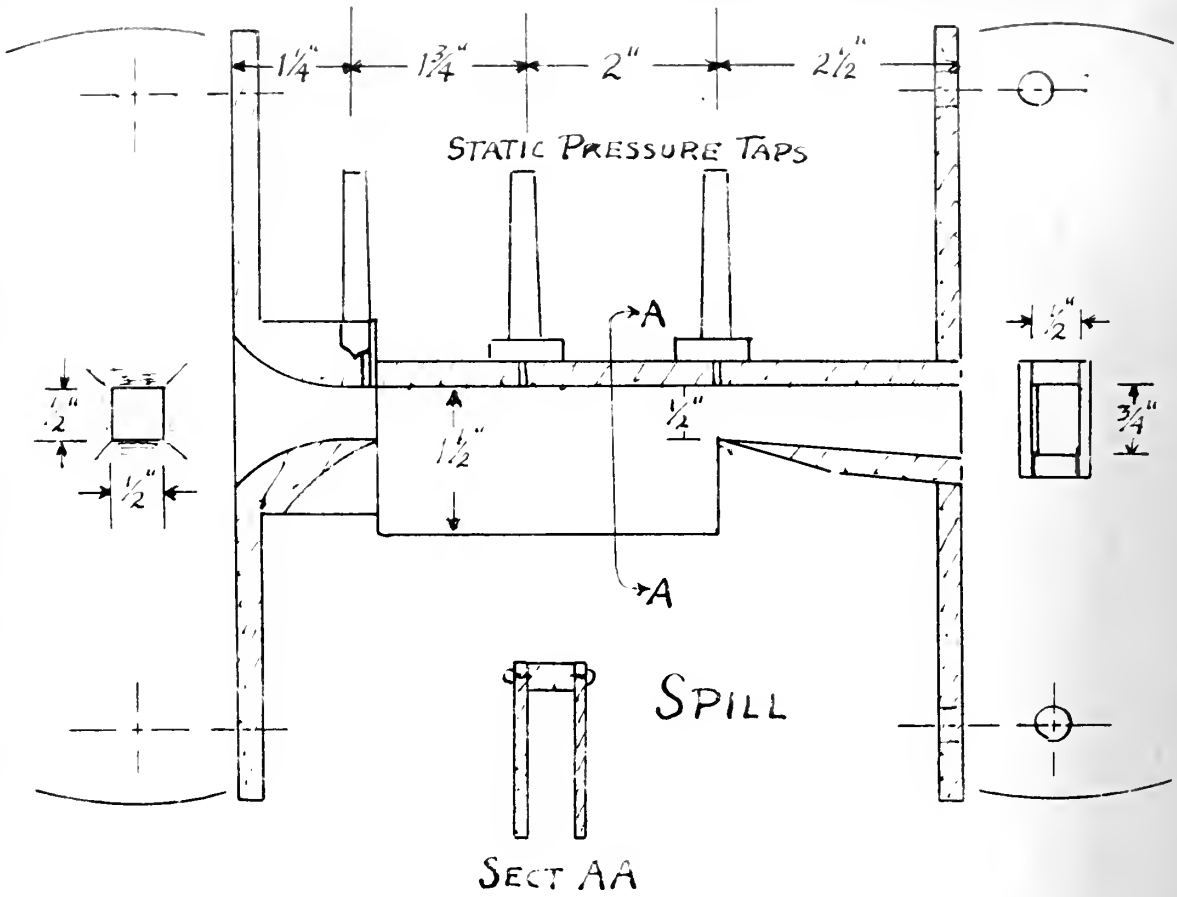

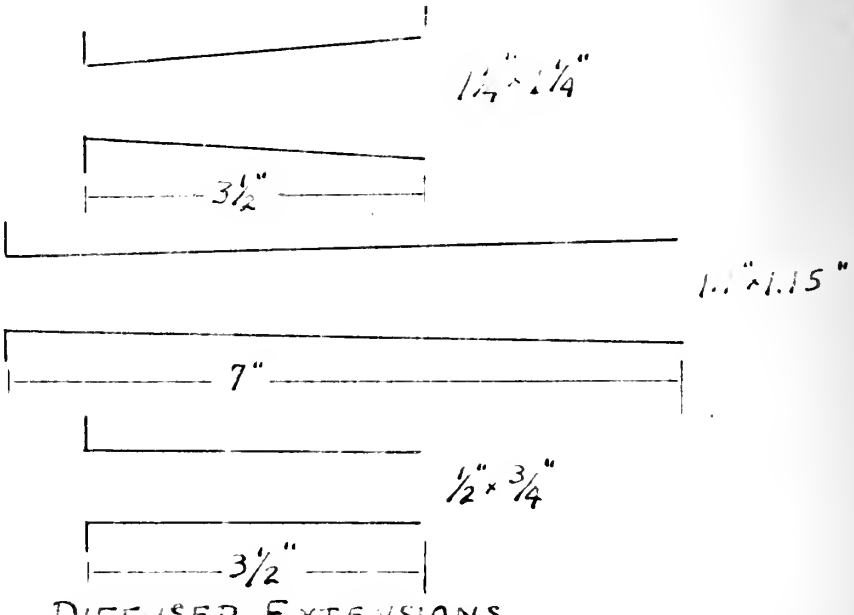

DIFFUSER EXTENSIONS

FIG 8

C.D. Winner 5/28/51

Figure No. 9

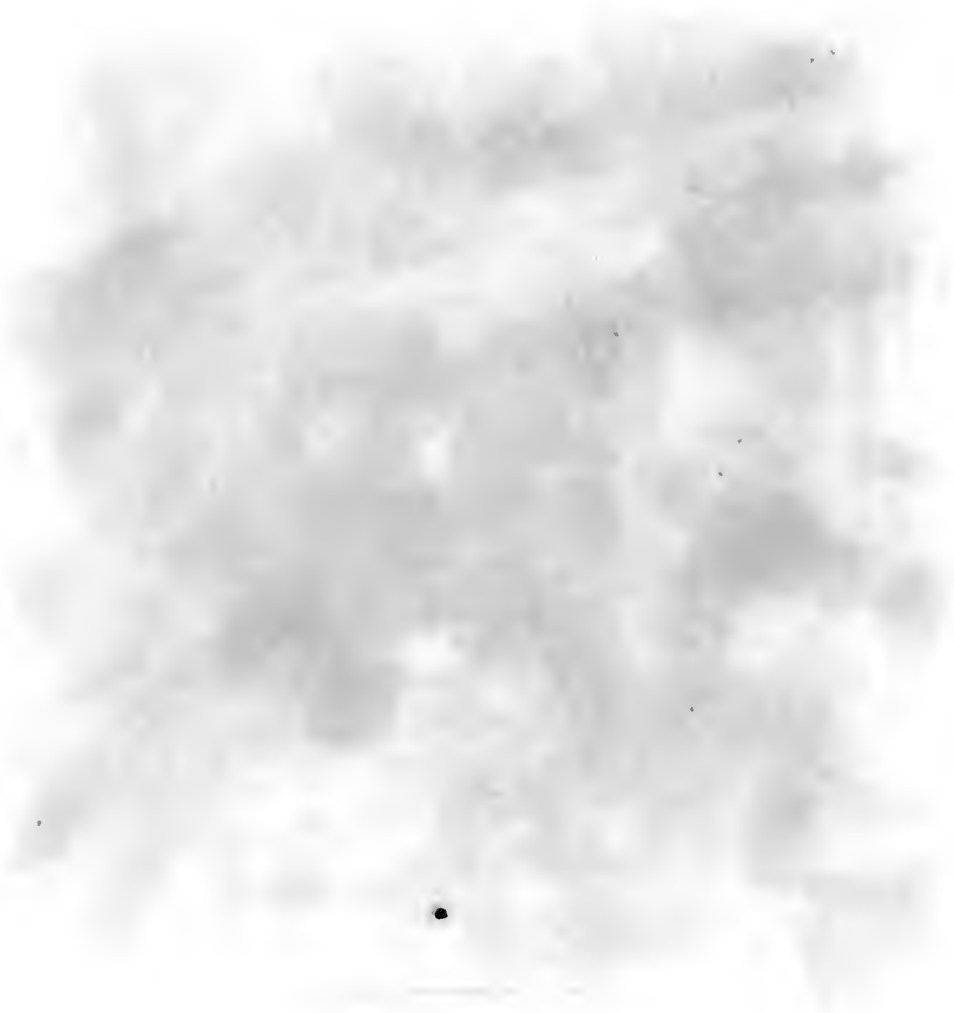

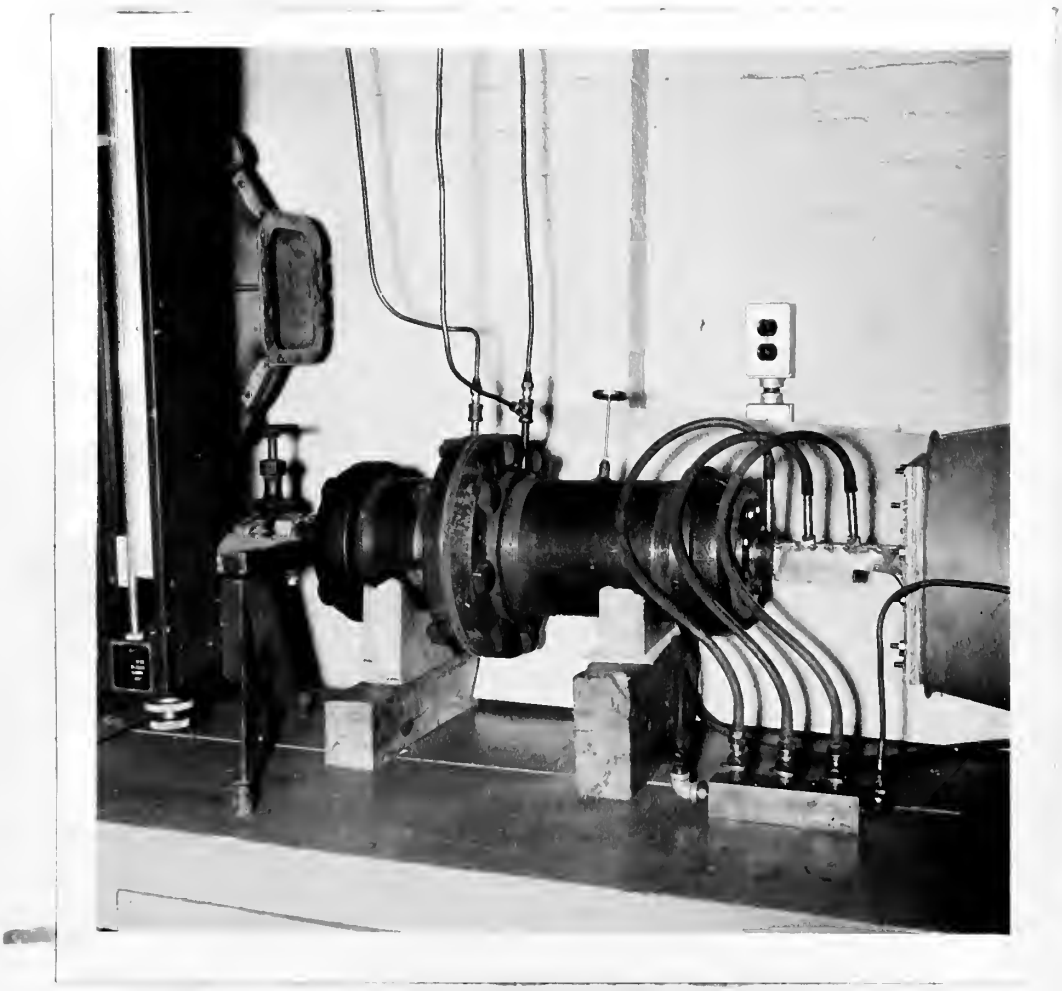

Figure No. 10

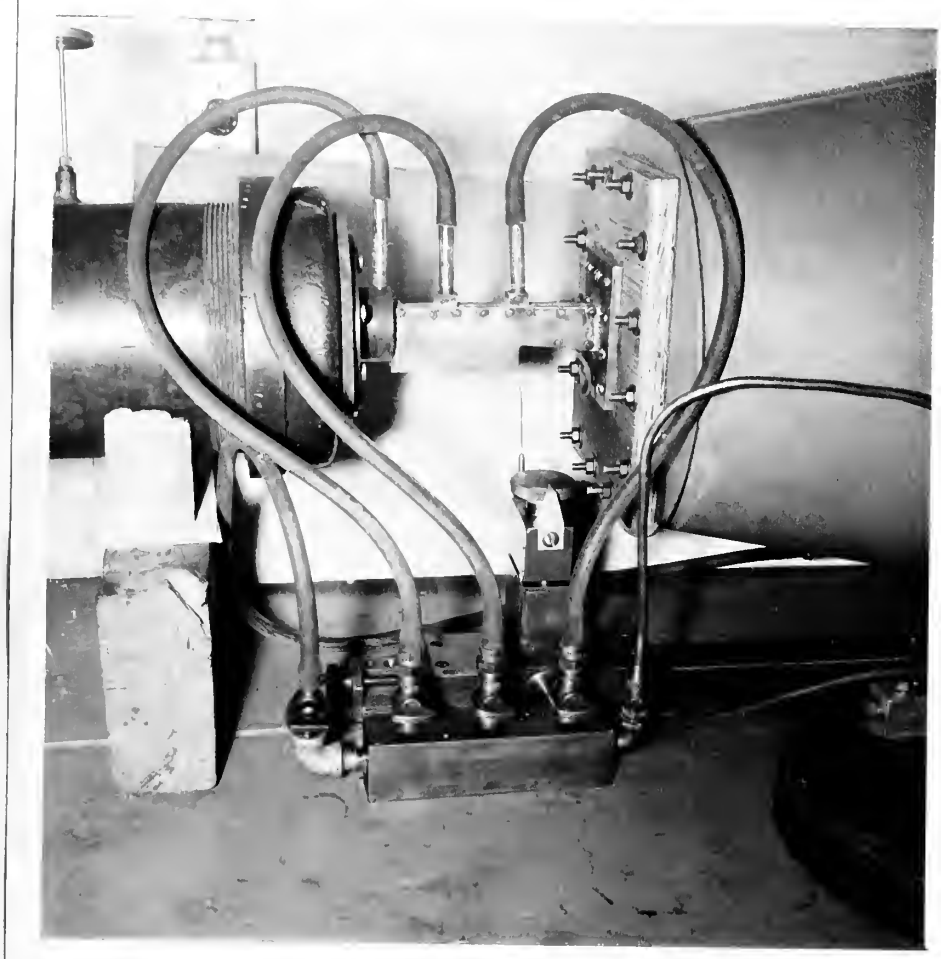

Figure No. 11

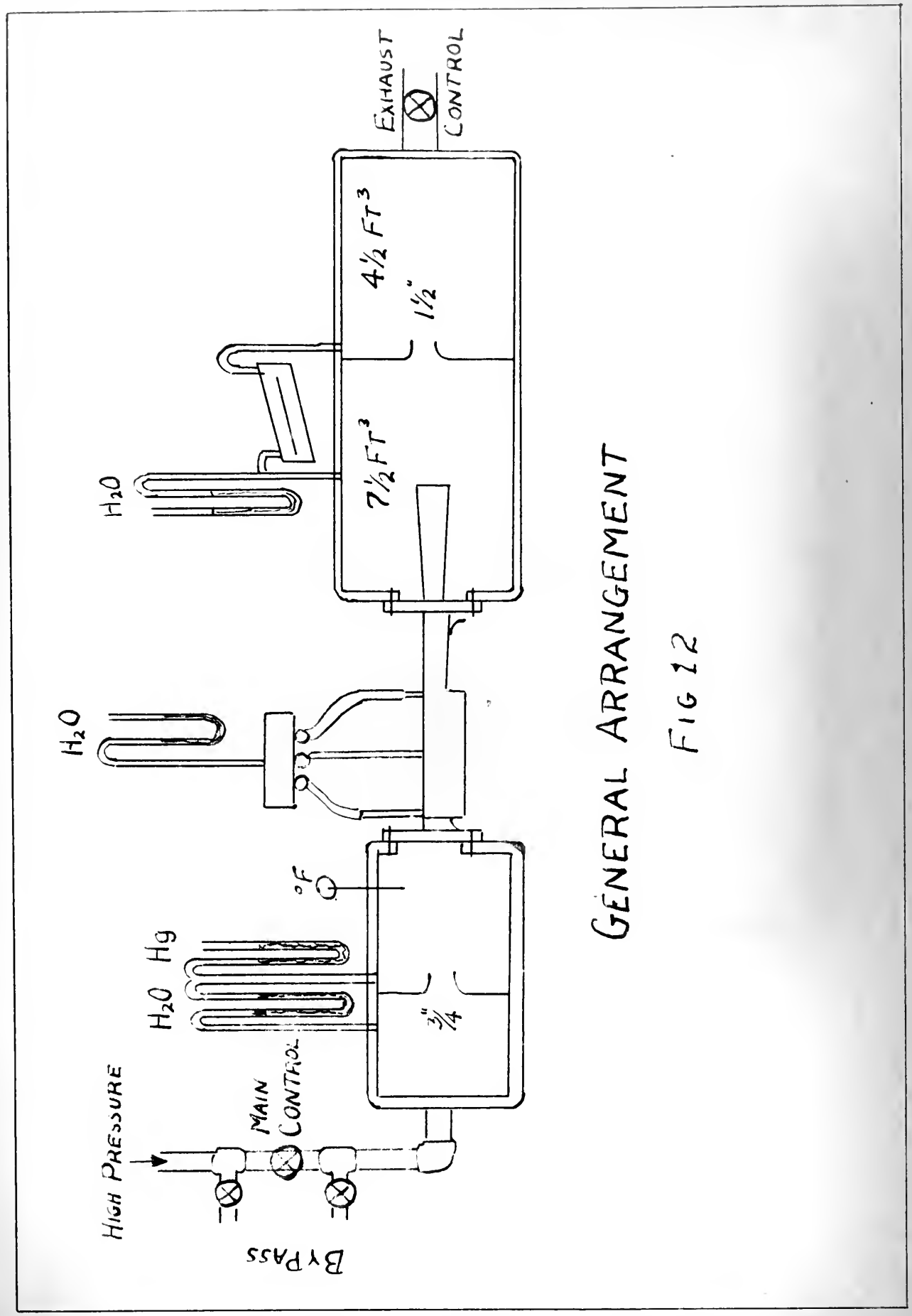

GENERAL ARRANGEMENT

FIG 12

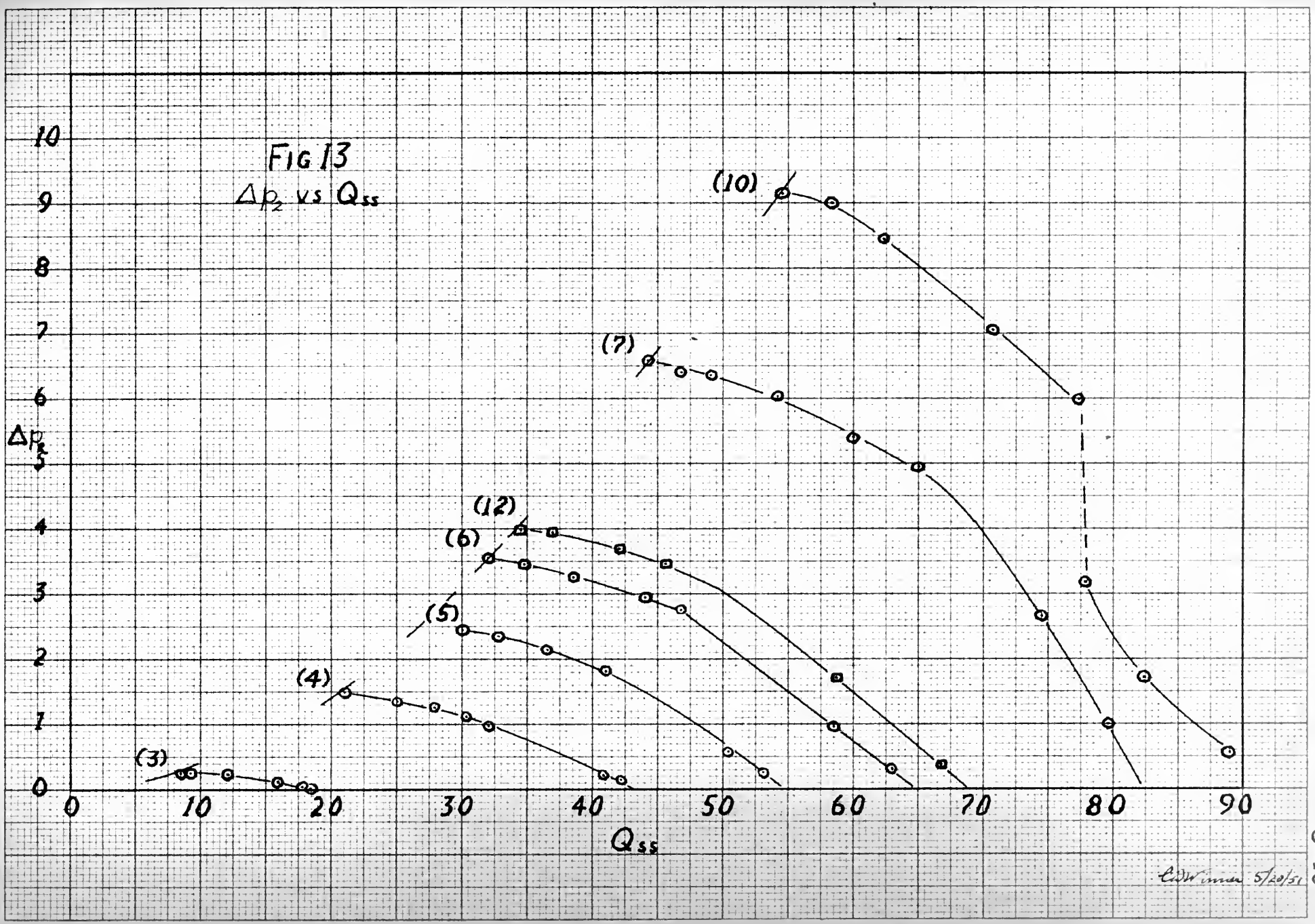
FIG 13
Δp_2 vs Q_{ss}
(10)
(7)
(12)
(6)
(5)
(4)
(3)
Δp_2
Q_{ss}
0
1
2
3
4
5
6
7
8
9
10
0
10
20
30
40
50
60
70
80
90
C.W. Inman 5/20/51

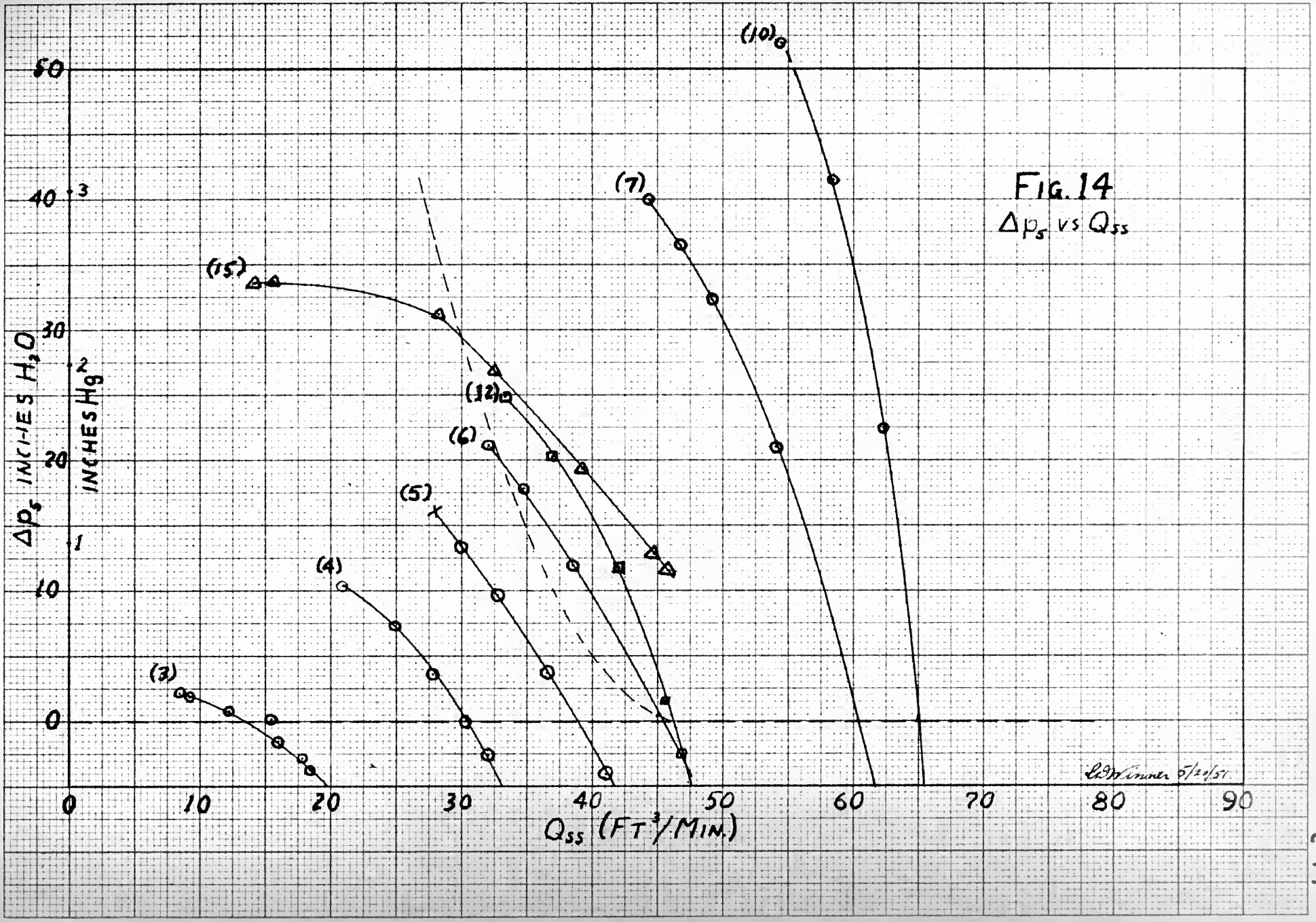
FIG. 14
Δp_s vs Q_{ss}
Δp_s INCHES H_2O
INCHES Hg
Q_{ss} (FT³/MIN.)
(3)
(4)
(5)
(6)
(7)
(10)
(12)
(15)
50
40
30
20
10
0
3
2
1
0
10
20
30
40
50
60
70
80
90
L.D. Kinner 5/20/51

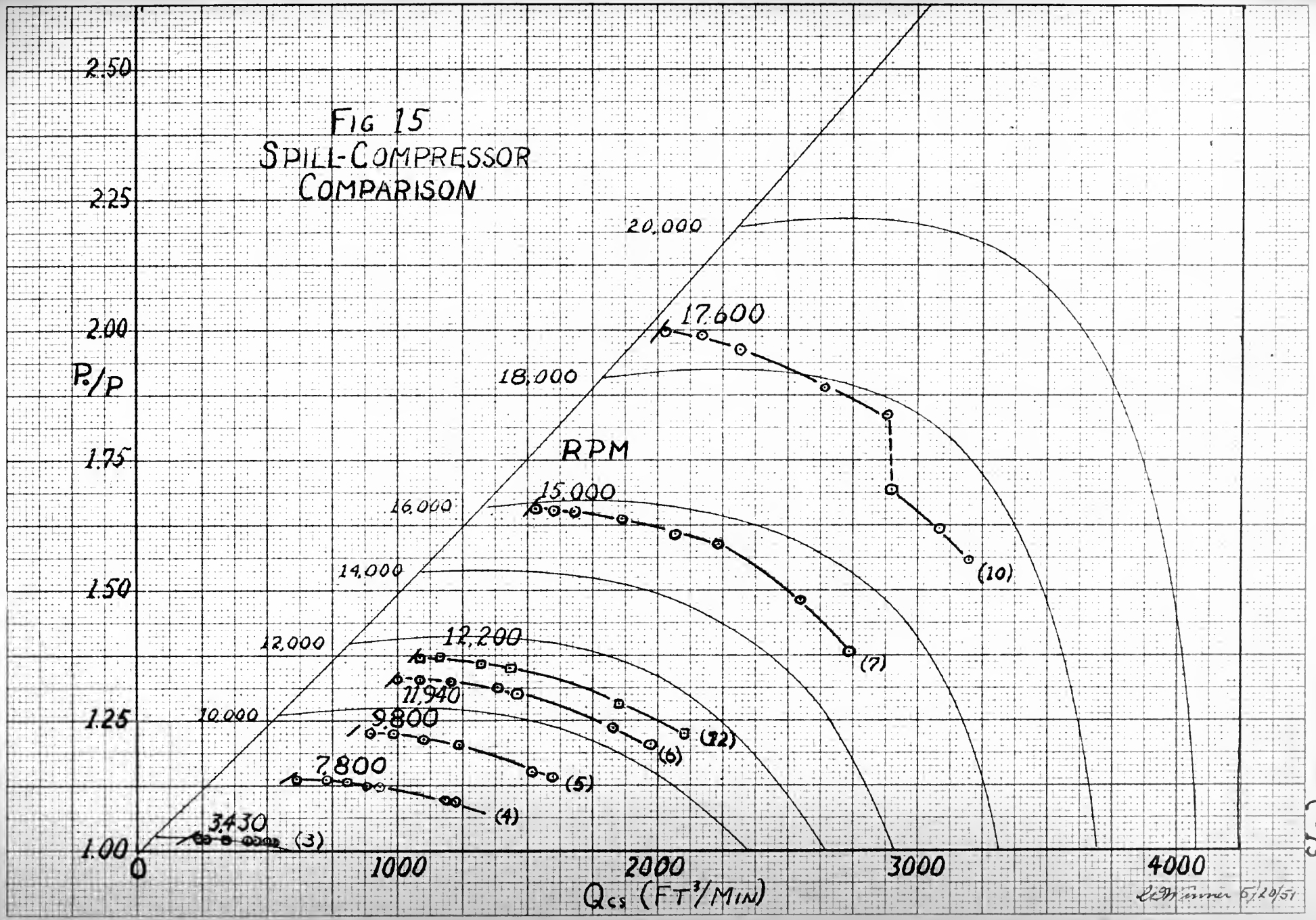
FIG 15
SPILL-COMPRESSOR
COMPARISON
2.50
2.25
2.00
P./P
1.75
1.50
1.25
1.00
0
1000
2000
3000
4000
Qcs (FT³/MIN)
RPM
20,000
17,600
18,000
15,000
16,000
14,000
12,200
12,000
11,940
10,000
9,800
7,800
3,430
(10)
(7)
(12)
(6)
(5)
(4)
(3)
L.C. Tanner 5/20/51

C-15

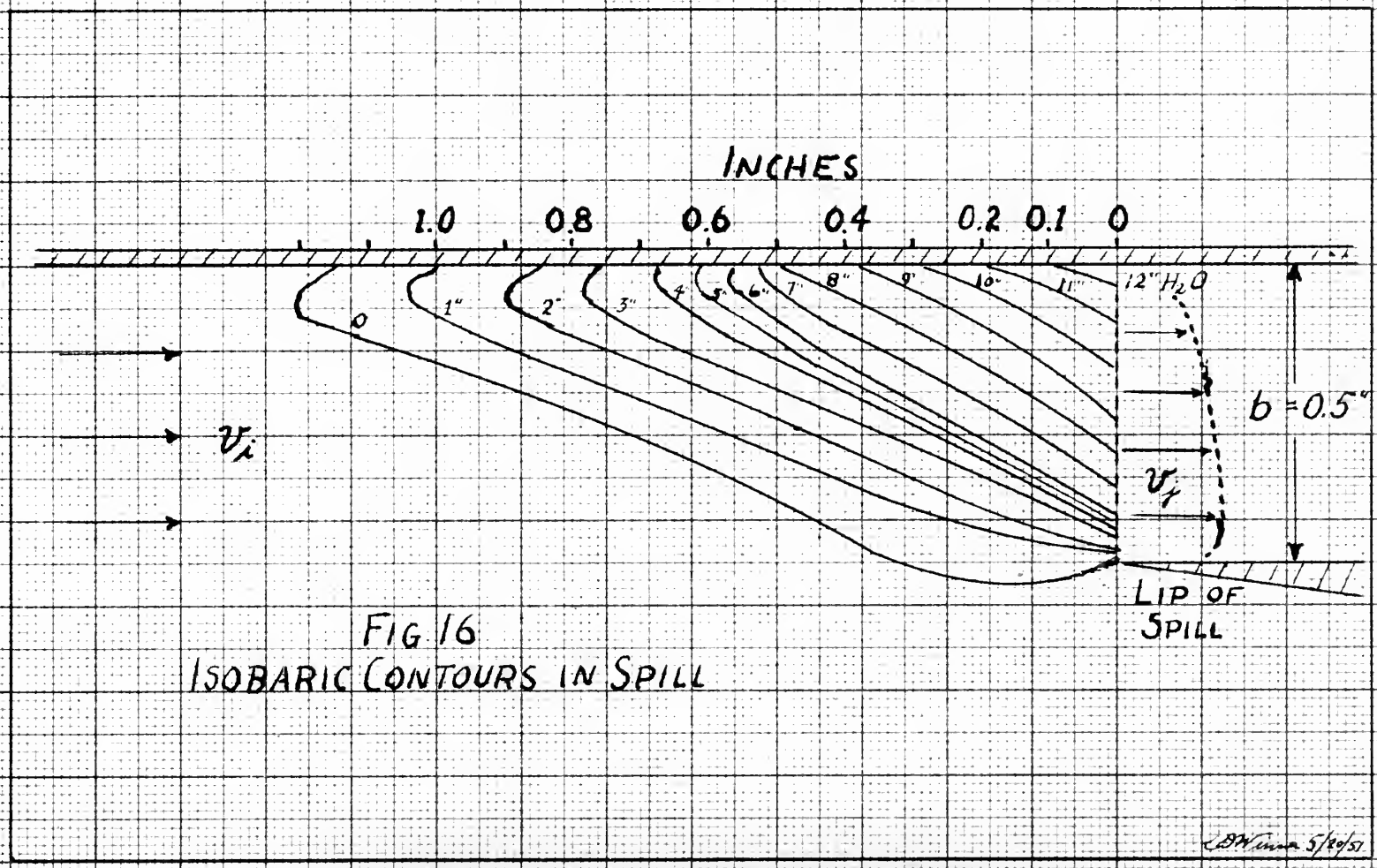

FIG 16
ISOBARIC CONTOURS IN SPILL

C-16

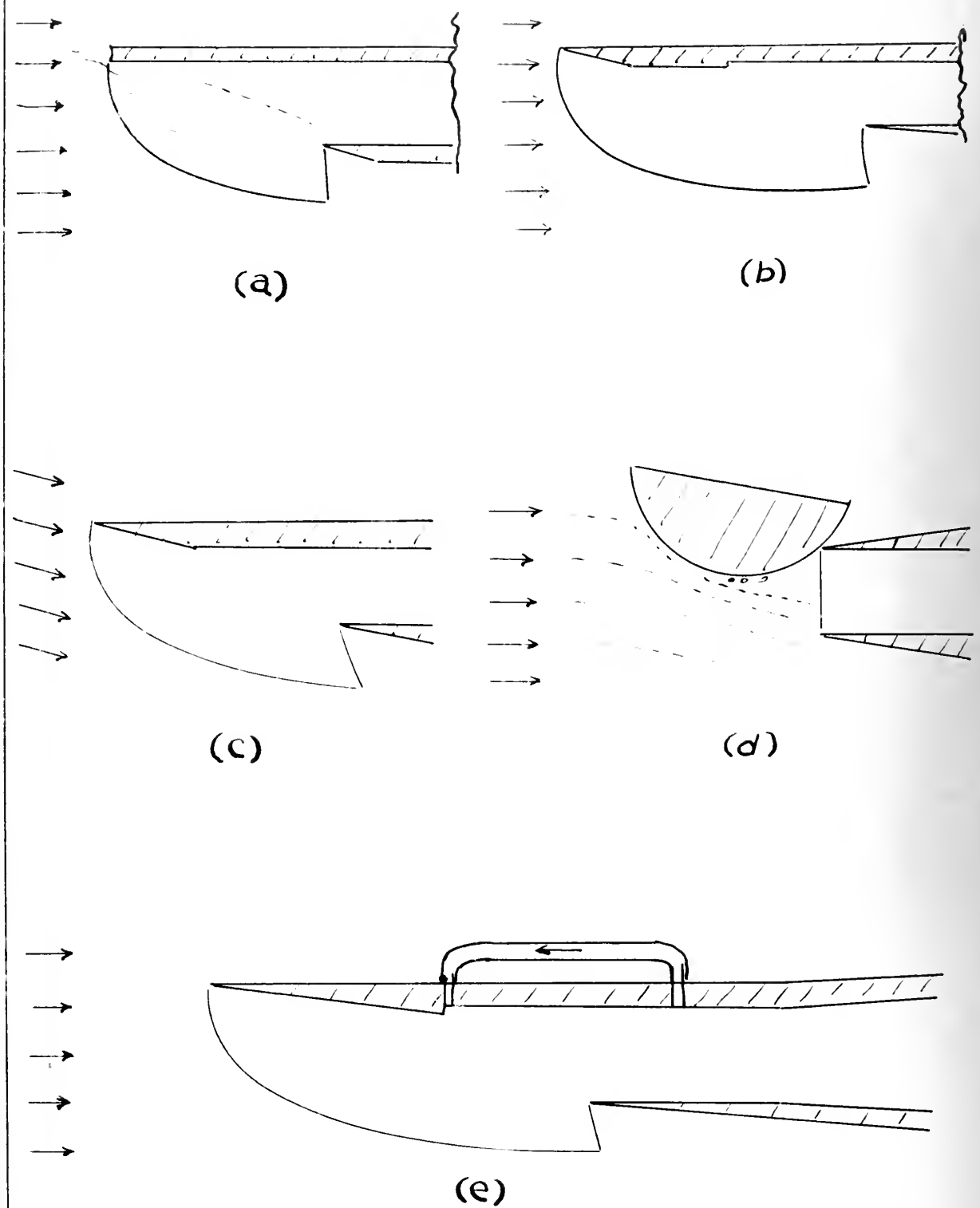

FIG 17

DEFLECTED SPILL PICKUP

L. W. Winner

5/23/51

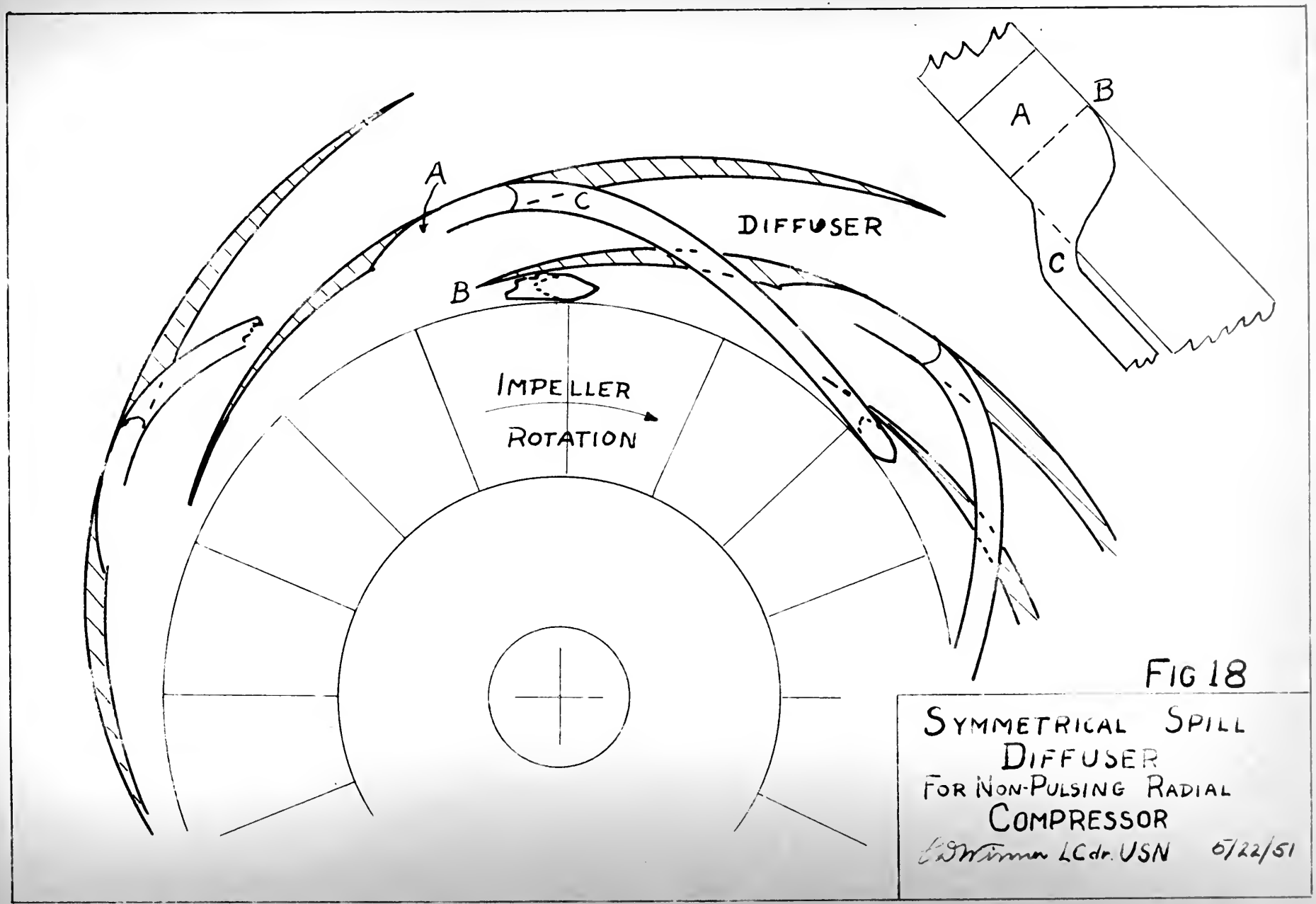

FIG 18

SYMMETRICAL SPILL DIFFUSER FOR NON-PULSING RADIAL COMPRESSOR

E.D. Trimm LCdr. USN 6/22/51

C18

TABLE I

Run No. 3 Δp_o = 0.50"Hg W_1 = .0219 lb/sec

Barometer = 29.72 Δp_1 = 2.09"H_2O v_i = 173 ft/sec

t_o = 90°F N = 3430 RPM

	Δp_2("Hg)	Δp_3("H_2O)	Δp_4("H_2O)	Δp_5("H_2O)	Δp_7("H_2O)
(1)	0	+0.19	+0.06	-3.16	0.14
(2)	0.04	↓	↓	2.78	0.13
(3)	0.06			-1.62	0.105
(4)	0.06			+0.02	0.10
(5)	0.13			0.73	0.06
(6)	0.12			1.95	0.035
(7)	0.13			3.10	0.03

	W_2 lb/sec	Q_s ft^3/min	p_o/p_3	p_2/p_b	$(p_2/p_1)_c$	Q_c ft^3/min
(1)	.0226	18.6	1.0168	1.0000	1.0168	521
(2)	.0218	17.9	↓	1.0013	1.0181	503
(3)	.0195	16.05		1.002	1.0188	450
(4)	.0190	15.65		1.002	1.0188	438
(5)	.0148	12.28		1.0044	1.0212	341
(6)	.0113	9.30		1.004	1.0208	261
(7)	.0104	8.56		1.0044	1.0212	240

TABLE II

Run No. 4 Δp_o = 2.5"Hg W_1 = .0496 lb/sec

Barometer = 29.72 Δp_1 = 10.3"H_2O v_i = 392 ft/sec

t_o = 103°F N = 7800 RPM

	Δp_2("Hg)	Δp_3("H_2O)	Δp_4("H_2O)	Δp_5("H_2O)	Δp_7("H_2O)
(1)	0.15	+1.07	-0.23	-19.00	0.71
(2)	0.21	x	x	16.9	0.665
(3)	0.98	x	x	2.54	0.400
(4)	1.12	1.10	0.10	0.00	0.355
(5)	1.27	x	x	+3.10	0.300
(6)	1.37	1.10	0.10	7.25	0.24
(7)	1.50	x	x	10.25	0.17

	W_2 lb/sec	Q_s ft^3/min	p_o/p_3	p_2/p_b	$(p_2/p_1)_c$	Q_c ft^3/min
(1)	.0503	42.2	1.0842	1.0050	1.0892	1228
(2)	.0487	40.8		1.0071	1.0913	1188
(3)	.0382	32.0		1.0330	1.1200	933
(4)	.0362	30.3		1.0377	1.1251	833
(5)	.0333	27.9		1.0427	1.1305	814
(6)	.0298	25.0		1.0461	1.1343	725
(7)	.0252	21.1		1.0504	1.1387	615

TABLE III

Run No. 5 Δp_o = 4.0"Hg W_1 = .0704

Barometer = 29.73 Δp_1 = 17.23"H_2O v_i = 493

t_o = 109°F N = 9,805

	Δp_2"Hg	Δp_3("H_2O)	Δp_4("H_2O)	Δp_5("H_2O)	Δp_7("H_2O)
(1)	0.25	1.80	0	-31.70	1.12
(2)	0.58	↓	↓	-25.55	1.00
(3)	1.82			- 4.05	0.64
(4)	2.13			+ 3.85	0.50
(5)	2.35			+ 9.6	0.40
(6)	2.45		+.05	+13.5	0.335

	W_2 lb/sec	Q_s ft^3/min	p_o/p_3	p_2/p_b	$(p_2/p_1)_c$	Q_c ft^3/min
(1)	.0630	53.1	1.1346	1.0084	1.143	1600
(2)	.0598	50.4	↓	1.0195	1.1565	1520
(3)	.0488	41.1		1.0612	1.203	1240
(4)	.0434	36.6		1.0716	1.215	1102
(5)	.0389	32.8		1.0790	1.224	988
(6)	.0356	30.0		1.0824	1.228	905

TABLE IV

Run No. 6 Δp_c=5.8"Hg W_1 = .0771

Barometer = 29.72 Δp_1 = 22.70"H_2O v_i = 600

t_o = 112°F N = 11,940

	Δp_2"Hg	Δp_3("H_2O)	Δp_4("H_2O)	Δp_5("H_2O)	Δp_7("H_2O)
(1)	0.33	+2.85	+0.45	(-)	1.58
(2)	0.98	↓	x	(-)	1.33
(3)	2.75	2.85	0.87	-2.65	0.805
(4)	2.95	2.80	↓	x	0.710
(5)	3.25	↓	↓	+11.90	0.54
(6)	3.45	↓	↓	17.65	0.44
(7)	3.55	↓	↓	21.20	0.37

	W_2 lb/sec	Q_s ft^3/min	p_o/p_3	p_2/p_b	$(p_2/p_1)_c$	Q_c ft^3/min
(1)	.0743	62.6	1.196	1.011	1.210	1970
(2)	.0692	58.0	↓	1.033	1.235	1828
(3)	.0554	46.5	↓	1.092	1.306	1463
(4)	.0522	43.7	↓	1.099	1.313	1380
(5)	.0457	38.3	↓	1.109	1.325	1206
(6)	.0413	34.6	↓	1.116	1.333	1092
(7)	.0380	31.9	↓	1.119	1.337	1005

TABLE V

Run No. 7 Δp_o = 10.8"Hg W_1 = 0.1185 lb/sec

Barometer = 29.70 Δp_1 = 36.4"H_2O v_i = 768 ft/sec

t_o = 114°F N = 15,220 RPM

	Δp_2"Hg	Δp_3("H_2O)	Δp_4("H_2O)	Δp_5("H_2O)	Δp_7("H_2O)
(1)	0.50	x	x	(-)	2.5
(2)	2.65	x	x	(-)	2.025
(3)	4.95	x	x	(-)	1.46
(4)	5.40	x	x	(-)	1.27
(5)	6.03	x	x	+21.0	0.98
(6)	6.36	x	x	32.2	0.80
(7)	6.40	x	x	36.4	0.725
(8)	6.60	x	x	40.0	0.65

	W_2 lb/sec	Q_s ft^3/min	p_o/p_3	p_2/p_b	$(p_2/p_1)_c$	Q_c ft^3/min
(1)	.0940	79.6	1.3635	1.0168	1.385	2740
(2)	.0875	74.1	↓	1.0891	1.485	2550
(3)	.0768	65.0	↓	1.1667	1.590	2240
(4)	.0710	60.1	↓	1.1818	1.610	2070
(5)	.0640	54.2	↓	1.203	1.642	1865
(6)	.0581	49.2	↓	1.214	1.656	1690
(7)	.0553	46.8	↓	1.2155	1.656	1610
(8)	.0525	44.4	↓	1.222	1.664	1530

TABLE VI

Run No. 10 Δp_o = 16.0"Hg W_1 = 0.0562 lb/sec

Barometer = 30.12 Δp_1 = 46.9("H_2O) v_i = 884 ft/sec

t_o = 112°F N = 17,600

	Δp_2"Hg	Δp_3("H_2O)	Δp_4("H_2O)	Δp_5("H_2O)	Δp_7("H_2O)
(1)	0.57	+10.1	+6.2	x	2.92
(2)	1.70	x	x	x	2.61
(3)	3.19	x	x	x	2.22
(4)	5.99	x	x	x	1.65
(5)	7.05	x	x	x	1.65
(6)	8.44	13.0	8.1	+22.5	1.24
(7)	9.00	13.0	8.5	41.5	1.07
(8)	9.15	13.0	x	52.0	0.93

	W_2 lb/sec	Q_s ft^3/min	p_o/p_3	p_2/p_b	$(p_2/p_1)_c$	Q_c ft^3/min
(1)	0.1030	89.0	1.532	1,0189	1.560	3200
(2)	.0990	82.4		1.0565	1.618	3080
(3)	.0934	77.8		1.106	1.693	2900
(4)	.0928	77.4		1.199	1.838	2880
(5)	.0848	70.7		1.234	1.890	2640
(6)	.0748	62.4		1.281	1.962	2325
(7)	.0700	58.4		1.299	1.990	2175
(8)	.0653	54.5		1.304	1.998	2030

TABLE VII (a)

Run No. 9 For 1st Pressure Probe Test

Barometer = 30.07 t_o = 110°F

	Δp_o ("Hg)	Δp_1 ("H_2O)	Δp_2 ("Hg)	Δp_3 ("H_2O)	Δp_4 ("H_2O)	Δp_5 ("H_2O)	Δp_7 ("H_2O)
(1)	5.8	23.3	3.55	x	x	+19.3	0.40

Static Pressure Survey Δp_{6s}

L* / n*	0	.2	.4	.6	.8	1.0
0	13.1	11.1	9.35	4.8	2.35	1.85
½	12.2	10.1	8.35	5.4	2.88	1.55
1	11.5	9.35	7.55	4.95	2.70	1.35
1½	-	8.85	7.05	4.35	2.35	0.75
2	10.45	8.35	6.45	3.75	1.60	0.40
2½	-	7.85	5.85	3.05	1.30	0
3	9.75	7.35	5.35	2.35	0.70	
3½	-	6.85	4.75	1.60	0	
4	9.00	6.20	4.15	0.85		
4½	-	5.45	3.45	0		
5	6.75	4.75	2.65			
5½	-	3.75	1.75			
6	5.60	2.75	0.95			
6½		1.65	0			
7		0.75				
7½		0				
8						

* L = Horizontal distance upstream from lip, inches.

n = Number of turns down from wall, 14 turns = 1 inch.

TABLE VII (b)

Run No. 11 For 2nd Pressure Probe Test

Barometer = 29.65 t_o = 110°F p_o = 5.8"Hg

	Δp_1 (H_2O)	Δp_2 ("Hg)	Δp_3 ("H_2O)	Δp_4 ("H_2O)	Δp_5 ("H_2O)	Δp_7 ("H_2O)
(1)	21.7	3.50	+2.65	+0.45	+19.5	0.40
(2)	21.9	3.50	+2.60	+0.55	+19.1	0.40

	(1) Static Pressure Δp_{6s} ("H_2O)		(2) Total Pressure Δp_{6t} ("Hg)			
L*	0	.16	.16	p_o/p_s	M	v
n*			Δp_{6t}			
0	19.65	16.45	3.73	1.121	.41	465
½	18.45	15.05	4.80	1.156	.46	522
1	18.05	14.55	5.13	1.167	.475	540
1½	-	14.00	5.34	1.174	.485	550
2	17.45	13.65	5.41	1.176	.488	555
2½	-	-	5.36	1.175	.486	552
3	17.25	12.90	5.30	1.173	.484	549
3½	-	-	5.15	1.168	.477	542
4	17.65	12.30	4.98	1.163	.470	534
4½	-	-	4.80	1.157	.461	523
5	18.45	11.10	4.58	1.154	.458	520
5½	-	-	4.35	-	-	-
6	20.15	8.90	4.10	1.135	.430	488
6½		6.30	3.93	-	-	-
7		3.80	3.53	1.118	.403	458
7½		2.20				
8		0				

* L = Horizontal distance upstream from lip, inches

n = Number of turns down from wall, 14 turns = 1 inch

TABLE VIII

Run. No. 12 Δp_o = 5.8"Hg W_1 = .0775

Barometer = 29.60 Δp_1 = 23.25"H_2O v_i = 614 ft/sec

t_o = 110°F N = 12,200

	Δp_2"Hg	Δp_3"H_2O	Δp_4"H_2O	Δp_5"H_2O	Δp_7"H_2O
(1)	0.38	-3.53	+3.08	(-)	1.74
(2)	1.72	3.35	3.15	(-)	1.30
(3)	3.47	3.35	2.95	+1.55	0.80
(4)	3.70	3.72	2.80	11.80	0.63
(5)	3.95	3.90	2.70	20.40	0.49
(6)	3.98	3.90	2.75	23.4	0.42
(7)	3.60	-3.90	2.75	25.0	0.40

	W_2 lb/sec	Q_s ft^3/min	p_o/p_3	p_2/p_b	$(p_2/p_1)_c$	Q_c ft^3/min
(1)	.079	66.4	1.208	1.0128	1.225	2100
(2)	.0695	58.4		1.0581	1.279	1850
(3)	.054	45.4		1.1172	1.350	1435
(4)	.0498	41.9		1.1249	1.360	1325
(5)	.044	37.0		1.1333	1.370	1170
(6)	.0408	34.3		1.1343	1.371	1086
(7)	.0395	33.2		1.125	1.360	1050

TABLE IX

Run No. 13 Δp_o = 0.6"Hg. W_1 = .0257 lb/sec

Barometer = 30.21 Δp_1 = 2.6 "H_2O v_i = 205 ft/sec

t_o = 85°F N = 4,090

	Δp_2("H_2O)	Δp_3("H_2O)	Δp_4("H_2O)	Δp_5("H_2O)	Δp_7("H_2O)
(1)	0.30	-0.15	+0.15	+1.17	.09
(2)	0.95	-0.11	+0.16	1.47	.078
(3)	1.67	↓	↓	2.00	.065
(4)	2.70	↓	↓	2.61	.050
(5)	4.22	↓	↓	3.50	.025
(6)	4.70	↓	↓	x	.015
(7)	4.91	↓	↓	3.78	.010
(8)	4.90	↓	↓	3.87	.005
(9)	4.80	↓	↓	3.87	0

TABLE X

Run No. 14 p_o = 4.1"Hg W_1 = .0686 lb/sec

Barometer = 30.20 p_1 = 18.40 "H_2O v_i = 500 ft/sec

t_o = 102°F

	Δp_2("H_2O)	Δp_3("H_2O)	Δp_4("H_2O)	Δp_5("H_2O)	Δp_7("H_2O)
(1)	3.30	-2.32	+1.48	+8.81	.60
(2)	4.51	-2.37	1.52	9.62	.57
(3)	9.05	↓	1.52	12.60	.485
(4)	14.08	↓	1.52	15.77	.400
(5)	23.80	↓	2.02	21.35	.235
(6)	28.2	↓	2.12	22.60	.150
(7)	30.95	↓	2.16	23.26	.100
(8)	32.95	↓	-	-	.060
(9)	34.15	↓	2.40	25.10	.040

TABLE XI

Run No. 15 Δp_o = 5.8"Hg W_1 = .0807 lb/sec

Barometer = 30.20 Δp_1 = 24.4 "H_2O v_i = 594 ft/sec

t_o = 110°F

	Δp_2 ("H_2O)	Δp_3 ("H_2O)	Δp_4 ("H_2O)	Δp_5 ("H_2O)	Δp_7 ("H_2O)	ΔW_2 lb/sec	Δv_2 ft/sec	ΔQ_s ft^3/min
(1)	+2.45	-3.53	+2.20	+11.50	0.85	.0551		
(2)	4.73	3.60	2.20	12.70	0.80	.0536		
(3)	15.60	3.76	2.25	19.31	0.60	.0471		
(4)	28.15	3.76	2.30	26.62	0.40	.0390		
(5)	34.25	3.76	2.53	30.13	0.30	.0340		
(6)	45.40	3.48	3.25	33.40	0.09	.0189		
(7)	45.50	-3.48	3.25	33.40	0.075	.0170		

References

1. "Steam and Gas Turbines" by Dr. A. Stodola, McGraw-Hill, New York, 1927

2. Educational Gas Turbine Performance, Installation and Operation, Bul. No. DF81523, General Electric, Aircraft Gas Turbine Division, West Lynn, Mass., 1946

3. Thermodynamics of High Velocity Flow, Professor Neil P. Bailey, Head of Department of Mechanical Engineering, R. P. I., Troy, New York, 1950

4. Gas Turbine Combustion and Stability, Professor Neil P. Bailey, Head of Department of Mechanical Engineering, R. P. I., Troy, New York, 1950

5. Stability in Flow With Heat Addition, Thesis by Robert Edelman, R. P. I., Troy, New York, 1951

SYMBOLS AND NOMENCLATURE

Symbol	Explanation	Units
A	Area	ft^2
A_c	Circumferential area of impeller rim	
A_i	Flow area in diffuser throat	
b	Distance from lip of spill to deflecting wall	ft
F	$\frac{W\sqrt{T_o}}{Ap}$	$\frac{^oF}{sec}$
g	Acceleration of gravity (32.17)	ft/sec^2
K	Percentage factor used with b	
L	Distance the deflecting pressure penetrates along the wall upstream from the lip of the spill	in.
M	Mach number $\frac{v}{\sqrt{\gamma gRT}}$	
N, n	Rotational speed	RPM
N_R	Reynolds number	
p	Pressure	lb/ft^2
Δp_o	Receiver pressure, guage	
Δp_1	Differential pressure, primary metering nozzle	
Δp_2	Plenum chamber, guage	
$\Delta p_{3, 4, 5}$	Spill, guage	
Δp_6	Pitot and static tube	
Δp_7	Differential, plenum chamber metering nozzle	
p_i	Compressor inlet	
p_b	Atmospheric (barometer reading)	
p_i	Static pressure in primary jet	
p_k	Dynamic pressure	

		Units
Q	Rate of flow	ft^3/min
	Q_D Designed rate of flow	
	Q_m Rate at p_2/p_1 max	
	Q_{min} Rate at initiation of instability	
	Q'_{min} $v_i A_i$	
R	Gas Constant (53.35)	ft lb/^oR
r	Radius of impeller	ft
T	Absolute temperature	^oR
	T_o Receiver, Total	
	T_1 Compressor inlet	
	T_i Primary jet	
v	Velocity	ft/sec
	v_e Average in diffuser throat	
	v_i of primary jet $\sqrt{v_t^2 + v_r^2}$	
	v_j Local velocities in jet stream	
	v_r radial component in compressor Q/A_c	
	v_t tangential component in compressor ωr	
W	Flow rate (weight)	lb/sec
	W_1 Primary jet	
	W_2 Flow to plenum chamber from spill	
γ	Ratio of specific heats = c_p/c_v = 1.395	
ρ	Density	$slugs/ft^3$